UNIVERSITY OF CALIFORNIA

SANTA CRUZ

TITLE

A dissertation submitted in partial satisfaction of the requirements for the degree of

DOCTOR OR PHILOSOPHY

in

CHEMISTRY

by

Carrie S. Tambo

September 2022

The Dissertation of Carrie S. Tambo is approved:

_____

Professor Seth M. Rubin, Ph.D., chair

_____

Professor Robert S. Lokey, Ph.D.

_____

Professor Needhi Bhalla, Ph.D.

_____

Peter Biehl

Vice Provost and Dead of Graduate Studies

Table of Contents

List of Figures

Abstract

Characterizing cell cycle Cdk mechanisms and the influence of Cdk inhibitors on cyclin assembly.

Carrie Tambo

The study of the cell cycle, specifically, understanding mechanistic regulation is fundamental for the development of therapeutic treatment in the event of disease. Limitless cell proliferation is a hallmark of cancer and often tied to cell cycle control. My research studied Cyclin-dependent kinases (Cdks) and their role in cell proliferation at the G1-S phase restriction point. I was able to shed insight on cyclin binding kinetics using Biolayer Interferometry (BLI) and the influence different types of inhibitors have on association of Cdks and cyclins. I reveal that Type I inhibitors increase binding affinity of CycA for Cdk2, whereas Type II inhibitors decrease affinity but differ in how they alter the CycA kinetic profile. Moreover, I explore an allosteric binding site of Cdk4-CycD that may be responsible for structural rearrangement to an active kinase configuration. My research as a whole gives insight into the development of a Cdk2 specific inhibitor and highlight the use of allosteric sites to understand mechanistic control of the cell cycle for Cdk inhibitor treatment therapy.

Acknowledgements

I want to give thanks to everyone who has provided their support for all these years. I have been fortunate to surround myself with compassionate people in graduate school and out. A huge shout out to my family, first and foremost, for always being there and offering their advice and guidance when I needed it. They believed in me from day one and always had, especially in times when I could not see it. My parents, Marcelo and Marina Tambo, taught me about discipline, perseverance, and to go after what makes me truly happy despite apprehensions. I also believe I could not have finished my thesis without my fiancé, Eric Silva. As my partner, he's been so patient, supportive, and always pushing me to be the best version of myself, which is something I still struggle with to this day. Graduate school has been a rollercoaster and in times where I let it take over, Eric has always been there to encourage me to take the reigns back.

I would like to thank the community that I have built in Santa Cruz. I moved here for graduate school and left with memories, life-long friends, and peers that I would never forget. I want to thank Seth Rubin for being my mentor and lab-dad. In times when I felt like I was not cut out for graduate school, he reminded me that I worked for it and earned my spot being there. My cohort, my lab mates, and friends made me feel at home and were my security blanket at times when I needed it. I would not have finished graduate school without the people that I have mentioned and for that I am so lucky to be surrounded by them.

Chapter 1

Cdks and what we know so far

The study of the cell cycle and the mechanisms that are responsible for its regulation are key fundamental processes to all living organisms. If we can understand the mechanistic regulations of cell cycle control, we can further understand major health conditions like cancer and developmental diseases.

A defining characteristic of cancer is its capability to proliferate uncontrollably and suppress mechanisms that identify and notify the cell of any major cell processes that are erroneous like incorrect cell size and DNA repair[1]. The cell cycle inherently has regulatory mechanisms put in place for quality control and the focus of my dissertation is on the G1-S phase restriction point. Transition for cells from G1 to S phase is a commitment step, meaning that once the cell has surpassed this point, the cell no longer requires external growth factors and can carry the cell through to completion of mitosis[2,3]. This G1-S restriction point is often deregulated and is a hallmark of cancer and this loss of regulation occurs through upregulation of important protein players called Cyclin-dependent kinases (Cdks) and/or loss of the Retinoblastoma tumor suppressor protein, Rb[1,4-6]. My following projects involve tackling one of the hallmarks of cancer, limitless cell proliferation, through the study of Cdks.

1.1 Structure and mechanism of Cdks upon activation

The cell cycle is a highly regulated process that occurs to ensure cells have grown to the correct size and have replicated their genome properly. Rb regulates the cell cycle at the G1-S phase transition and is invariably inactivated in all types of cancer[1-5]. Rb maintains and halts the cell in the G1 phase by binding and suppressing activating transcription factor E2F, a family of

transcription factors responsible for transcribing downstream cell cycle genes for entry into S phase. Transition into the S phase involves the process of Rb inactivation through phosphorylation of Rb by Cdks in complex with their cyclin binding partners. Cdks control progression through the cell division cycle and are prominent targets for cancer therapeutics due to their impact on proliferation as Rb is commonly inactivated in tumor cells by Cdk phosphorylation[2,3]. Cdks coordinate processes throughout the cell cycle by phosphorylating protein substrates to change their localization, stability, and binding interactions[4,5,7].

There is a wide variety of Cdks and cyclins that act in a timely and controlled manner to keep proper regulation of cell cycle progression[4]. The phosphorylation event of Rb happens in a positive feedback loop and in a sequential manner with initial phosphorylation by Cdk4/6-CycD due to expression of D-type cyclins in early G1 phase. In late G1, CycE is expressed and forms a complex with Cdk2 to allow for full phosphorylation of Rb. Cdk2 can also bind to CycA, a homolog of CycE, and acts later on Rb in the S phase to sustain full Rb phosphorylation and is responsible for other critical DNA replication processes. Cdk1-CycB acts as a mitotic phase activator at the G2-M phase transition. All of these Cdk-Cyc complexes act together in keeping the controlled regulation of the cell cycle[5].

Based on structural data of Cdks, they are commonly composed of an N-terminal lobe (N-lobe) of mainly beta sheets and a C-terminal lobe (C-lobe) of alpha helices. In the N-lobe lies several structural important contacts: an ATP-binding site, C-helix, activation loop (A-loop), and DFG motif; some of which structurally rearrange themselves to allow for binding of cyclin subunits, substrate binding and phosphorylation, and to accommodate designer inhibitors. The cell-cycle Cdks are activated by binding of the cyclin subunit and phosphorylation of a specific threonine in the kinase A-loop, which shift the kinase from an inactive to an active state. The structural changes that occur upon cyclin binding and A-loop phosphorylation reposition the C-helix and

A-loop to generate a conformation optimized for ATP binding, substrate binding, and catalysis [4,5,8,9].

The principles of structural rearrangement of Cdk activation and cyclin association have been heavily studied in Cdk2-CycA[9]. To fully understand the mode of Cdk activation, we first must understand Cdk architecture when unbound to its cyclin. Cdks are inherently in the inactive state in their monomeric form due to the configuration of the A-loop not being phosphorylated at the conserved threonine residue, Thr160 on Cdk2. Here, I use Cdk2 as an example and when inactive, the A-loop occludes the active site preventing the binding of ATP and does not allow for substrate binding and thus catalysis. Here, I want to highlight residue Glu51, a conserved catalytic site residue, as it is important in the cyclin bound Cdk2, but in the free Cdk2 monomer Glu51 remains outside the active site and solvent exposed. The A-loop is positioned in such a way that it is solvent exposed and accessible, containing the phosphoacceptor Thr160, to be phosphorylated for Cdk activation. Due to the positioning of the A-loop, the C-helix points out and away from the kinase[8,9].

Activation of the Cdk happens through association of the cyclin binding partner followed by phosphorylation of the phosphoacceptor at Thr160. Several binding events occur to allow for an active Cdk2-CycA complex. Upon CycA association, there is nearly a 90º rotation and ~9 Å shift of the C-helix inwards towards the active site is due to the movement of Pro45 at the start of the C-helix. The C-helix of Cdk2 gets surrounded by several hydrophobic interactions and movement of the C-helix reposition the conserved catalytic residue, Glu51, into the active site. This allows the coordination of ATP binding important for catalysis of protein substrates by orienting the phosphate groups of ATP. CycA association binds the A-loop in such a way that it relieves the blockade the A-loop creates at the entrance of the active site through the displacement of the αL12 helix with a β-sheet (residues 150-152) on Cdk2[8]. The addition of the phosphate group on Thr160 makes several contacts with the C-helix and within the A-loop

itself. The phosphate group makes contacts with arginine residues as a means of neutralizing the negative charge. Two residues I want to point out that aid in neutralizing the phosphate are Arg50 of the C-helix and Arg150 within the A-loop of Cdk2, as these make important interactions with CycA at residues Phe267 and Glu268, respectively. Direct contacts are made between Thr160 and CycA through several van der Waals interactions. There is an increase in the hydrogen bond network seen in the phosphorylated Cdk2-CycA dimer.

Inactivation of Rb by Cdk phosphorylation is required for S phase entry and is commonly deregulated in proliferating cancer cells[10]. Cancerous cells are incapable of responding to growth suppressors and sustain proliferative and replicative ability. Moreover, overexpression of one or any of these Cdks or cyclins can cause imbalance in cell cycle control. For example, the D-type cyclins are often overexpressed in many tumor types and results in hyperactivity of associated kinases Cdk4/6[11]. The deregulation of Cdk pathways in cancer has motivated significant research into the development of Cdk inhibitors as therapeutics[12,13].

1.2 The journey of developing specific Cdk inhibitors

This prompted the need for therapeutic strategies and gave rise to drugs that were developed to target these upregulated Cdks in cancer disease. Around the year 2000, the first generation of Cdk inhibitors were developed and released into clinical trials. Roscovitive and flavopiridol are two examples of broad-spectrum inhibitors for Cdks, but due to this multi-target activity, there was a lack in adequate efficacy and safety. Consequently, the second generation of Cdk inhibitors entered clinical trials around 2010 with more selectivity and this included the drugs dinaciclib and CR8. Dinaciclib, for example, specificity was increased for Cdk2 and Cdk5, but in the end, these second generation Cdk inhibitors, had tolerable doses but efficacy at these doses are not as effective for solid tumors or advanced breast cancer. One of those off-targets were Cdk1 which is essential for cell cycle function; therefore, it is critical that Cdk1 be excluded

as a drug target as knockout of Cdk1 cannot be rescued by Cdk2[14]. Moreover, knockout of Cdk1 in mice do not generate viable mice and in cells, embryonic fibroblasts arrest in G2. Moreover, Cdk1 and Cdk2 have a high degree of active site sequence identity making it hard to discriminate between the two active forms of the kinases[15]. Overall, pan-Cdk inhibitors proved to be too toxic with their generalized Cdk inhibition and promiscuity resulting in off-target effects[16].

The success of palbociclib, the first Cdk4/6 specific inhibitor, and related Cdk4/6 inhibitors in the clinic is motivating evidence that intervention in cell-cycle control pathways is a viable strategy for reducing cancer progression[17,18]. Currently, palbociclib and similar compounds ribociclib and abemaciclib are available in the clinic to treat advanced breast cancer[19,20]. Palbociclib works by competing with ATP for binding to Cdk4/6-cyclinD heterodimers. We know that palbociclib can target Cdk4/6 monomer and dimer with the D-type cyclin isoform CycD1. Previously in the Rubin Lab, it was shown that palbociclib was unable to inhibit p27-Cdk4-CycD1 trimer activity to phosphorylate Rb, indicating that palbociclib targets are unclear[20].

Efforts in the development of similar inhibitors have been progressing with several others currently in clinical trials, but a difficulty of these inhibitors is their rapid turnover in developing resistance, therefore, bypassing drug effectiveness[16]. There is steady evidence that show sensitivity and resistance to Cdk4/6 inhibitors after some time after treatment[21]. Since the administration of palbociclib has been used as a cancer treatment, growing evidence show that prolonged treatment of palbociclib have induced acquired resistance and decreased sensitivity. For instance, treatment of palbociclib to ER-positive breast cancer cell lines beyond 24 hours showed the return of baseline levels of phosphorylated Rb[21]. Cdk4/6 inhibition is limited in that early adaptations are made that circumvent Cdk4/6 inhibition. One approach is through Cdk2 activity as expression of its cognate CycE partner becomes amplified as a response to Cdk4/6 inhibition, resulting in Cdk2 activation[22]. Additionally, since D-type cyclins are overexpressed

in these advanced breast cancer cases, it was also shown in a coimmunoprecipitation experiment that Cdk2 and CycD1 were pulled down together upon treatment of palbociclib[21]. This rescued Rb phosphorylation by a noncanonical Cdk2-CycD complex explains the decrease in sensitivity and demonstrates one possible mechanism that cancer cells develop resistance of Cdk4/6 inhibitors. For this reason, there has been a growing interest in specifically targeting Cdk2 because it can compensate and trigger S-phase entry upon Cdk4/6 inhibition[21].

The development of small molecule kinase inhibitors can be classified by their mode in which they bind. Here, I focus on a subset; Type I inhibitors bind the active kinase conformation and Type II target the inactive confirmation that results in the outward flip of the conserved tripeptide motif DFG. In the context of Cdk inhibition, a panel of Cdk inhibitors have differential binding capacities for Cdk1/2 and their cyclin-bound counterparts, indicating clear differences between Cdk inhibitors for their proposed target and possibly using this discrepancy as an advantage for drug development[23]. The fact that Cdks can exist in varying confirmations and can bind other proteins adds layers of complexity to what Cdk inhibitors specifically target. Therefore, this prompts a need for the identification of protein targets of Cdk inhibitors.

My studies show the influence Cdk inhibitors have on Cdk-cyclin interactions and give insight into the continued development with the purpose of restoring regulation of the cell cycle, as well as provide insight on additional scaffolds for drug targets. Understanding how Cdk inhibitors work and identifying their limitations in their targets are essential for future drug development and being able to expand the work of Cdk inhibitors to be more efficient, effective, and specific.

Chapter 2

A biolayer interferometry assay for Cdk-cyclin association reveals diverse effects of Cdk2 inhibitors on cyclin binding kinetics

We report here a biolayer interferometry (BLI) assay that enables facile quantification of Cdk binding interactions with their cyclin activators. We applied this assay to measure the impact of Cdk2 inhibitors on Cyclin A (CycA) association and dissociation kinetics. We found that Type I ATP active site inhibitors increased CycA affinity for Cdk2 by slowing the CycA dissociation rate. In contrast, Type II and other inhibitors that bind preferentially to inactive Cdk2 monomer had varying effects on the association and dissociation processes to decrease CycA affinity. We propose that the different impact of inhibitors on the cyclin binding kinetics arise from the structural perturbations they impart on the activation loop and C-helix of the Cdk, which form key cyclin binding interfaces. Our assay and results will be beneficial for further study of Cdk-cyclin interactions and for designing inhibitors that disrupt Cdk-cyclin assembly.

2.1 Biolayer interferometry (BLI) assay for measuring Cdk2-CycA binding kinetics

The Cdks that control the cell cycle are often found in cells with specific cognate cyclin partners; for example, CycD pairs with Cdk4 and Cdk6, while CycA and CycE pairs with Cdk2. Although these Cdks and cyclins have been extensively studied along with additional protein inhibitors and activators in the complex, the molecular determinants of these preferential enzymatic pairings and differences in intrinsic activities remain unclear. Recent studies have also brought attention to the significance of noncanonical pairings and activators. These noncanonical pairings occur in the context of proliferating cancer cells, which may have imbalanced levels of Cdks, cyclins, or their regulators[19], in situations in which a Cdk is genetically inactivated[22], and in the context of Cdk inhibitor treatment, which may alter the distribution of subunits in Cdk

complexes[20,21,24,25]. Despite the impact of Cdk-cyclin association on the cell cycle and proliferation, there have been few studies that quantify Cdk-cyclin affinity to understand the factors that drive and modulate binding and their binding preferences[14,26-28].

On the other hand, the intrinsic and acquired resistance of cancers to Cdk4/6 inhibitors points to the need for development of molecules towards other targets, especially Cdk2, which can compensate for Cdk4/6 and is often a primary driver of cancer cell proliferation[29]. While the approach to Cdk inhibitors has focused on competitive inhibitors that bind the ATP site, other approaches have been explored and may be particularly useful toward development of Cdk2 inhibitors. Creating specific Cdk2 inhibitors that target the ATP binding site in the active kinase conformation (Type I) has been challenging due to structural homology with Cdk1[23,30]. Cdk1 inhibition in most contexts results in toxicity, which is consistent with past observations that knockout of Cdk1 does not generate viable mice[31,32]. Interestingly, several Type I inhibitors discriminate in their binding between monomeric Cdk2 and Cdk1, while most of that selectivity is lost when targeting the active Cdk-cyclin heterodimers[23]; these observations suggest that targeting monomeric Cdk2 can be specific. There has also been reports of a Type II inhibitor, AUZ 454 (or K03861), which binds monomer Cdk2 and stabilizes an inactive conformation of the A-loop DFG motif[33], and of a class of compounds developed specifically to inhibit Cdk2-cyclin association[34,35]. Another recent study found that the plant alkaloid and approved drug for leukemia known as homoharringtonine (HHT) inhibits Cdk2-CycA association and promotes autophagic degradation of Cdk2[36]. These alternative approaches to targeting Cdk2 rather than active Cdk2-cyclin complexes, and, more broadly, Cdk inhibitor design in general would benefit from understanding how inhibitor-kinase association impacts cyclin association and vice-versa. Interestingly, a recent study has demonstrated that inhibitor and cyclin binding are thermodynamically coupled due to the impact of both on the C-helix and A-loop conformation[37].

Here we describe a biolayer interferometry (BLI) assay for measuring Cdk-cyclin binding, and we directly quantify the affinity and kinetics of Cdk2-CycA association. We then tested the effects of different classes of Cdk2 inhibitors and found both positive and negative effects of different drugs on association and dissociation kinetics. Remarkably, we find that molecules can inhibit CycA binding through different kinetic mechanisms, and we use structural insights to explain how drug perturbations to the conformation of the C-helix and A-loop impact the CycA binding interactions. Our assay and findings will be useful for the future development of Cdk2 specific inhibitors.

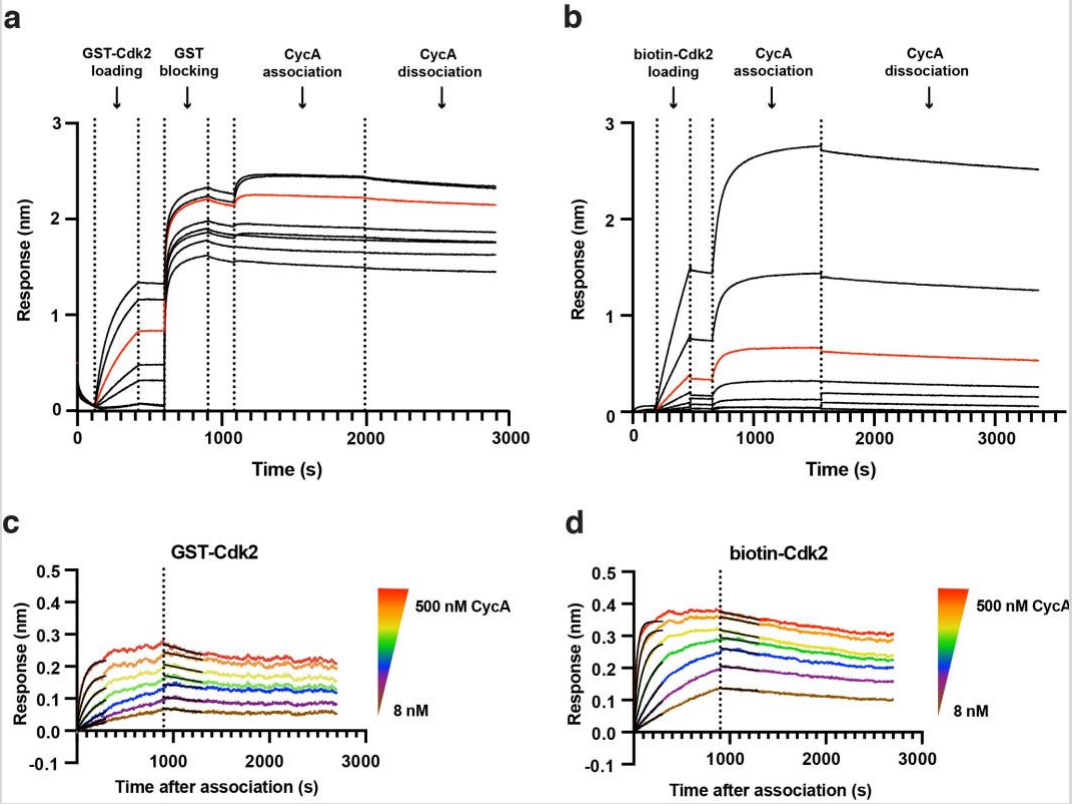

Figure 1: Biolayer Interferometry (BLI) assay measured kinetics of Cdk2-CycA binding. (a and b) Full unprocessed BLI sensorgrams that show response as a function of experiment time. The different curves represent different Cdk2 loading concentrations. The experiment with the concentration used in subsequent experiments (750 ng/mL GST-Cdk2 and 750 ng/mL biotin-Cdk2) is shown in red. (c and d) Association and dissociation steps of BLI assays using GST-Cdk2 (c) and biotin-Cdk2 (d). The concentration of CycA is varied in these experiments, and each sensorgram is double-referenced by subtracting both a zero ligand (Cdk2) and zero analyte (CycA) sensorgram.

We developed a BLI assay to measure Cdk2-CycA interactions. BLI enables observation of association and dissociation kinetics, is high throughput, and requires minimal quantities of purified reagents (~100 ng per assay)[38,39]. In the BLI format, the smaller protein (here Cdk2) is immobilized onto the biosensor through an affinity tag. Upon dipping the loaded biosensor into an analyte (CycA) solution, analyte binding is detected as a real-time interferogram throughout the duration of the experiment. We attempted Cdk2 immobilization using either a GST fusion

protein tag or a biotinylated preparation of the enzyme at various concentrations and found that 750 ng/mL was optimal to detect changes in response while preventing saturation of the sensor (Figure 1a,b). For GST fusion, Cdk2 was cloned and expressed in *E. coli* with a GST affinity tag, which was used both for protein purification and for immobilization through use of an anti-GST biosensor. For biotinylation, the GST fusion tag was cleaved during purification, and the Cdk2 was covalently modified with an N-terminal biotinylated peptide using the sortase enzyme[40]. Biotinylated Cdk2 was immobilized in our assays with streptavidin biosensors. When using either immobilization strategy, we found that nonspecific binding (NSB) was a reoccurring issue. NSB was observable as a BLI response that occurred upon dipping an empty biosensor, i.e. not loaded with Cdk2, into CycA solution. The NSB was remedied by the addition of 2 mg/mL BSA and 0.2% Tween to the assay running buffer, and in the case of using the anti-GST biosensors, by the insertion of a blocking step using 1 μM GST to block any accessible sites on the biosensor.

For both the GST-Cdk2 and biotin-Cdk2 experiments measuring CycA binding kinetics, the immobilized ligand on the biosensor was dipped into analyte at different concentrations. A range of CycA concentrations from 500 nM to 8 nM, in two-fold step dilutions, yielded data with optimal response signal and variation in k_{obs}, which is the observed rate constant during the association step (Figure 1c,d). We monitored association of CycA by the increase in BLI response for 900s, but we found that the entire range of data does not fit well to a single kinetic step. We suspect that there is a second slower process that is either nonspecific binding or a slower specific binding event that is coupled to a structural transition in either Cdk2 or CycA. For simplicity, we focused our analysis on the fast association step that had a much greater response, and we determined k_{obs} and the maximum response by fitting the first 300s of data to a single k_{obs}. To measure dissociation rate constants (k_d), the immobilized Cdk2 was dipped in buffer and dissociation of CycA was detected through the decrease in BLI response. For the dissociation step, we fit the first 400s of data and determined the k_d by assuming that the

response returns to zero. Fitting the data in this manner, we determined similar values of k_d, the association rate constant (k_a, determined from k_{obs} and k_d), and binding constant (K_d) for both differentially immobilized Cdk2 constructs. The maximum response for immobilized biotin-Cdk2 biosensor was consistently greater than for immobilized GST-Cdk2 biosensor when compared at similar protein concentrations, and we also observed less variation in the fit parameters across the different concentrations and replicates for the biotin-Cdk2 experiments. We obtained similar binding parameters when Cdk2 was phosphorylated on its activation loop by Cdk-activating kinase prior to purification (Figure S1). Therefore, for all subsequent studies, we used the unphosphorylated biotin-Cdk2 immobilized on the biosensor.

2.2 Cdk2 inhibitors change CycA association and dissociation rates

We applied the optimized BLI assay to study the influence of Cdk2 small molecule inhibitors on the kinetics of CycA association and dissociation. Considering the allosteric coupling that has been observed between structural features of the Cdk2 kinase, including the C-helix and activation loop, and CycA binding[37], we hypothesized that Cdk2 inhibitors could influence the kinetics of cyclin assembly by stabilizing different Cdk2 structural conformations. A panel of Cdk2 inhibitors that vary in their pharmacophore and their mode of action was used along with palbociclib, a Cdk4/6 specific inhibitor, as a negative control (Figure 2). In one approach, we introduced a high concentration of each drug (2 µM) at the baseline step in the BLI assay that occurs after loading Cdk2 but before addition of CycA (i.e. at ~500 sec in Figure 1b), and 2 µM of each drug was present during subsequent steps. 2 µM was chosen based on reported kinase activity inhibition constants, and the intention was to keep a saturating concentration of drug during the association and dissociation steps such that the experiments reflected only the kinetics of CycA binding to drug-bound Cdk2 complexes. We did not detect a BLI response when the Cdk2 biosensor is introduced to drug alone during the preincubation step, suggesting

that under our assay conditions, the signal is not sensitive to the subtle changes in the molecular weight or conformation induced by drug binding to kinase alone.

We observe changes in the affinity and kinetics of CycA binding for all of the tested drugs, apart from the negative control palbociclib, which does not bind Cdk2 at the tested concentration (Figure 2)[14]. We tested two Type I Cdk2 inhibitors that bind the active conformation of the kinase at the ATP site. Dinaciclib is a pan-Cdk inhibitor that targets Cdk1/2/5/9[41], while BMS265246 targets Cdk1/2/4[42]. We found that the Type I inhibitors significantly increased the affinity (smaller K_d) of CycA binding to Cdk2, around 3-fold for dinaciclib and 6-fold for BMS265246 (Figure 2a,b,f). For both drugs, the increase in affinity occurs through a decrease in the dissociation rate constant k_d, while the k_a is not significantly different. The observation of cooperativity between Type I ATP-site inhibitors and CycA binding had been previously observed through comparison of inhibitor affinities for Cdk2 alone vs. Cdk2-CycA complexes[37]. Here, we demonstrate the same cooperativity through direct measurement of CycA affinity and show that it manifests through a slowed dissociation.

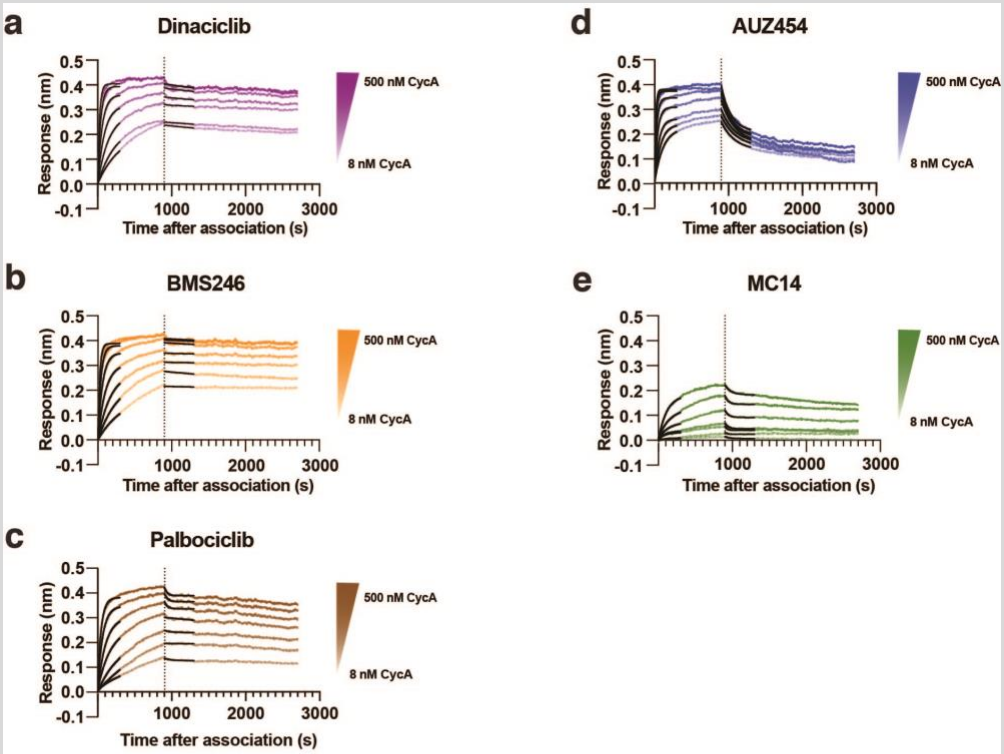

f

	k_a (x 10^4 $M^{-1}s^{-1}$)	k_d (x 10^{-4} s)	K_d (nM)
No drug	11 ± 6	1.7 ± 0.2	1.9 ± 0.8
Dinaciclib	14 ± 7	0.7 ± 0.2*	0.6 ± 0.3*
BMS246	14 ± 8	0.4 ± 0.2*	0.3 ± 0.1*
AUZ454	30 ± 10*	50 ± 10*	20 ± 10*
Palbociclib	11 ± 2	1.3 ± 0.5	2.2 ± 1.5

* $p < 0.0001$, comparison to no drug

Figure 2: BLI assays measuring the effects of inhibitors on CycA binding kinetics. (a-e) In each experiment, biotin-Cdk2 was immobilized at a concentration of 750 ng/mL and CycA concentration is varied as in Figure 1c,d. 2 μM drug was added to the buffer during the equilibration step preceding CycA addition and maintained throughout the association and dissociation steps. The set of sensorgrams in each panel shows the CycA association and dissociation steps of each BLI experiment. Each set corresponds to one of two replicate experiments performed under each condition. The rate and dissociation constants were calculated by averaging fit parameters from all the sensorgrams corresponding to different CycA concentrations in both the performed replicates (14 sensorgrams), and the standard deviation is reported as error. (f) Table summarizing fitting of kinetic data.

We tested two compounds in the assay that are known Cdk-cyclin assembly inhibitors (CCAIs). We found using the BLI assay that AUZ 454, which binds preferentially to monomeric Cdk2 over Cdk2-CycA[34], significantly decreased CycA affinity by ~10-fold (Figure 2d and 2f). Interestingly, AUZ 454 influences both the association and dissociation steps. AUZ 454 increased both k_a and k_d, but the relatively greater increase in k_d results in a weaker K_d. The nearly ~30-fold faster dissociation is particularly striking, and in the presence of AUZ 454, the dissociation curves could be fit without assuming return to zero signal. We suspect the residual signal is from nonspecific interactions, some of which may be protein aggregation. Other potential CCAIs have been reported that are not canonical Type II inhibitors in that they do not induce an inactive conformation of the DFG motif[35,36]. We tested Merck compound 14 (MC14), which is a quinoline-based compound developed from a screen of CycA binding inhibitors[35]. It was previously reported that MC14 binds Cdk2 with 5 nM affinity, as determined from temperature dependent circular dichroism, and destabilizes purified Cdk2-CycA complexes as determined by thermostability experiments[35]. In the presence of 2 mM MC14, we found a decreased response for CycA association across the CycA concentration range (Figure 2e). This observation suggests that MC14 occludes CycA association and that the residual signal is generated from the population of drug-free kinase on the biosensor.

2.3 Measuring Cdk2 inhibitor and ATP dose response on CycA association

We next adapted the BLI assay to measure dose responses of the drugs by maintaining the CycA concentration at 125 nM and varying drug concentration across the eight biosensors in an experiment (Figure 3). As in the CycA titration experiments, drug was introduced to immobilized Cdk2 for 180 seconds after Cdk2 loading on the biosensor and prior to exposure to CycA, and drug was maintained in solution during CycA association and dissociation. Using this approach, we assume that a drug-concentration dependent equilibrium with Cdk2 is present for the duration of the experiment such that the observed rates only depend on the

specific kinetics of CycA binding. In support of this assumption, experiments using longer 30 minute preincubation times showed similar results (not shown). As we titrated the Type I inhibitor BMS265246, the slope of the dissociation curve noticeably flattens and the k_d decreases (Figure 3a). We found that the dynamic range of the k_d change was rather limited to extract a precise K_i, but we found an IC_{50} ~ 10 nM. We tested AUZ 454 in the dose response format and also found we could measure the drug-dependent changes in k_d (Figure 3b). We fit the dose response curves to determine IC_{50} for CycA inhibition and used our measured K_d for Cdk2-CycA association to calculate corresponding K_i values. We emphasize that these K_i values quantify the potency of the drug in inhibiting CycA binding to Cdk2 (rather than catalytic activity). We found a similar but slightly tighter K_i value for AUZ 454 ($K_i = 10 \pm 7$ nM) compared to the previously reported K_d value for Cdk2 (50 ± 4 nM)[34]. In the dose response experiment with MC14, increasing drug concentration correlated with a lower BLI response in a dose-dependent manner (Figure 3c). Our interpretation is that CycA cannot associate with the fraction of Cdk2 on the biosensor that is bound by drug and the remaining drug-free Cdk2 associates with CycA with the same binding kinetics as observed in the absence of drug. We found a slightly weaker MC14 K_i for CycA inhibition compared to the previously reported affinity of MC14 for Cdk2 ($K_d = 5$ nM)[35]. Unlike the drugs, titration of ATP or the mimetic ATP-gamma-S did not generate any changes to the kinetics of CycA binding (Figure S2). We also tested the reported Cdk2-CycA inhibitor homoharringtonine (HHT) in the dose response assay format, but we found no strong effects at concentrations as high as 32 mM HHT (Figure 3d). We also could not observe any heat signal above background when titrating HHT with Cdk2 in an isothermal titration calorimetry experiment (Figure S3), so we found no evidence of HHT-Cdk2 interaction.

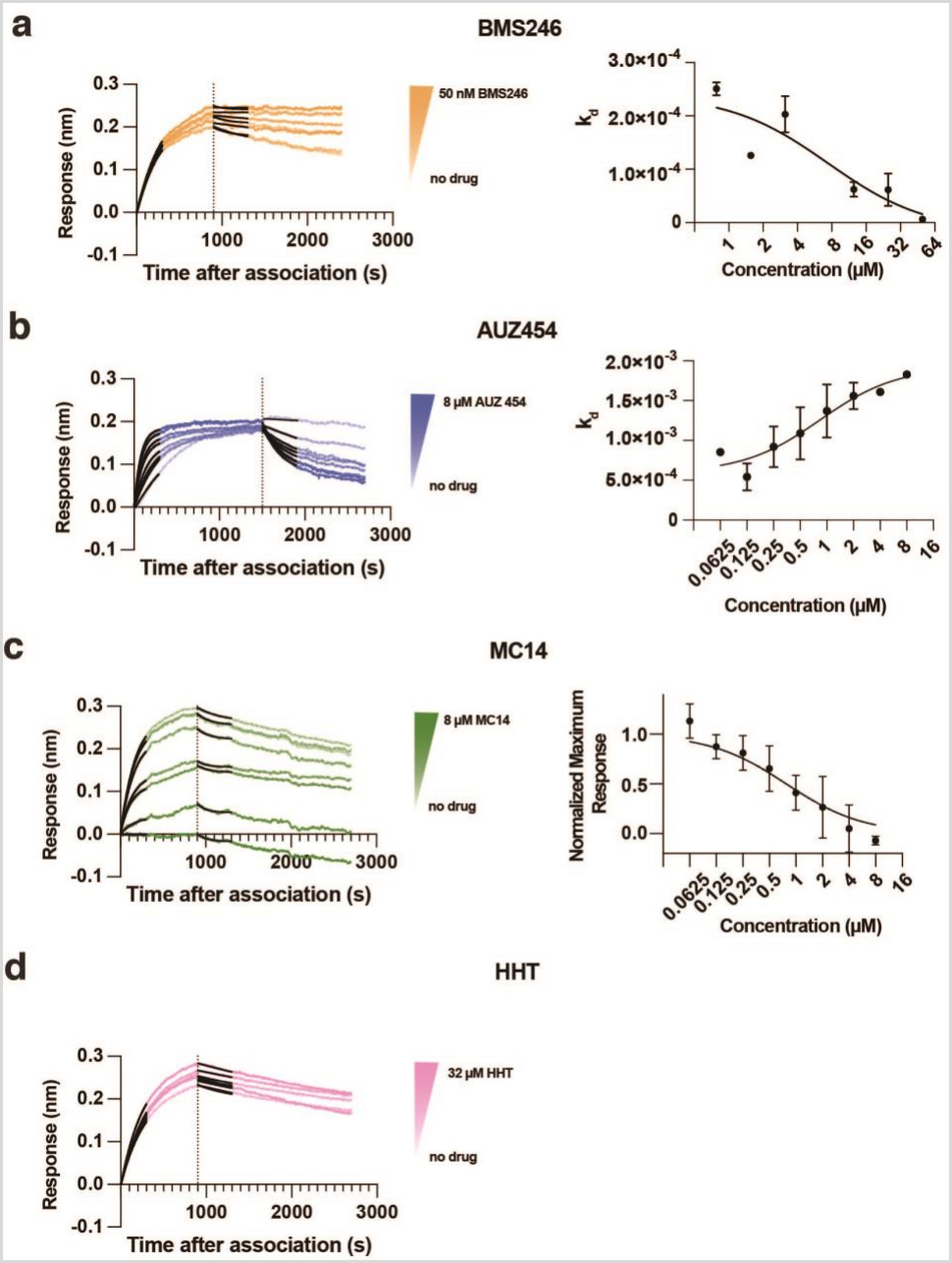

Figure 3: Dose response BLI measurements of Cdk2 inhibitors and ATP. The indicated Cdk2 inhibitor was varied and the CycA concentration is kept fixed at 125 nM. Dose response curves are plotted at right. Average values for the maximum response (normalized to the maximum response in the absence of drug) or k_d at each concentration across three replicates are plotted, and the error bars correspond to the standard deviation.

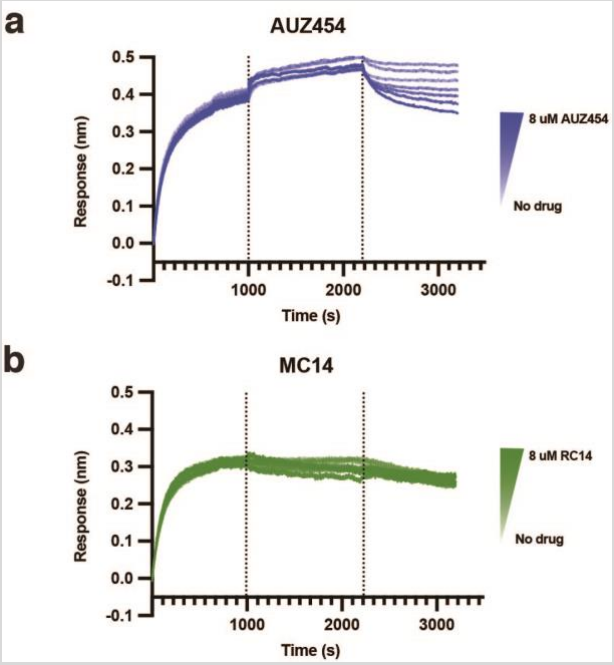

Figure 4: Effects of Cdk2 inhibitor when CycA added first to Cdk2. Dose response of (a) AUZ 454 and (b) MC14 when Cdk2 is exposed to drug (middle step) only after CycA association (left step). CycA is kept in the middle step with drug and then removed for dissociation (right step).

We tested in the dose response format the impact of exposing CCAIs to a preformed Cdk2-CycA complex, rather than incubating drugs with Cdk2 prior to CycA association (Figure 4). In these experiments, Cdk2-loaded biosensors were dipped into wells of CycA only (Figure 4, left step), then into CycA with drug to allow for drug incubation in the presence of CycA (middle step), and then into drug only to allow CycA to dissociate (right step). In the titration with AUZ 454, we observed little change in response during the co-incubation period (Figure 4a, middle step) and an increase in the CycA dissociation rate when CycA is removed (Figure 4a, right step). This result is consistent with our interpretation that AUZ 454 forms a ternary complex with Cdk2-CycA but stimulates CycA dissociation. In the presence of CycA in the middle step, CycA dissociates and re-associates with the Cdk2 biosensor, as the overall equilibrium favors the ternary complex in presence of high CycA concentrations in solution relative to the K_d. However, once CycA is removed from solution, the Cdk2-CycA-Auz 454 ternary complex is both kinetically and thermodynamically labile, and the remaining CycA on the biosensor dissociates. When CycA was introduced prior to MC14 (Figure 4b), we observe no change during the co-incubation period and CycA dissociation kinetics resemble CycA dissociation in the absence of drug. This observation supports the conclusions that CycA and MC14 binding

are incompatible and mutually exclusive and that CycA dissociation is sufficiently slow such that MC14 cannot bind Cdk2 during the co-incubation period.

2.4 Structural rearrangements are responsible for differences in cyclin association in the presence of Cdk inhibitors

We used available and new structural data to understand the basis for the different effects of the CCAIs on CycA binding kinetics. In particular, we were interested in identifying any structural perturbations of the drugs binding to monomer Cdk2 that may explain why AUZ 454 increases both k_a and k_d, while MC14 decreases k_a such that we could not detect the association signal. Comparison of the AUZ 454-Cdk2 structure (PDB ID: 5A14) with the apoCdk2-structure (PDB ID: 1HCK) reveals a significant rotation and shift of the C-helix that is induced through specific interactions with the drug (Figure 5a)[33,43]. Specifically, Leu55 in Cdk2 makes van der Waals contacts with the terminal trifluoromethylphenyl ring and the sidechain of Glu51 in the C-helix makes two hydrogen bonds with the NHs on the urea linker that connects the terminal trifluoromethylphenyl ring with the 4-amino-phenyl ether scaffold. These interactions move the C-helix more than 6 angstroms towards the “in” conformation relative to apoCDK2, which places Leu55 and Glu51 in nearly the same positions as in the active Cdk2-CycA structure (PDB: 1FIN) (Figure 5b)[8]. We propose that the increase in k_a results from the priming effect of AUZ 454 on the C-helix in that it properly positions the C-helix for CycA association. Notably, the interactions made by AUZ 454 and Cdk2 are for the most part compatible with the CycA-bound structure (Figure 5b), explaining why we still observe significant affinity of CycA in the presence of the drug. The main exception is that the position of the sidechain of F148 in the DFG motif in the active Cdk2-CycA structure clashes with the terminal trifluoromethylphenyl ring of AUZ 454 in the AUZ 454-Cdk2 structure. There is no available structure of AUZ 454 bound to Cdk2-CycA complex, and beyond a few residues that

follow the DFG motif, the activation loop is not ordered in the AUZ 454-Cdk2 structure. We propose that the perturbation to the activation loop conformation, which in the active structure makes a number of stabilizing contacts with CycA, is the likely source of the increase in the k_d. We also note that the b-sheet in the N-terminal lobe of the kinase domain is rotated slightly away from CycA in the AUZ454-Cdk2 structure compared to the apoCdk2 structure (Figure 5a). While the source of this rotation is not obvious, it may be another reason why the cyclin dissociation is more rapid.

We determined the structure of MC14 bound to Cdk2 by soaking crystals of apoCdk2 with compound (Table S1, Figures 5c,d). As previously observed for the similar compound MC2, MC14 binds the hinge at the ATP site through its hydroxyl group on the 4-OH-phenyl, and the chloro group on the 4-Cl-styryl extends toward the C-helix and contacts residues in the C-helix and A-loop (Figure S4). Importantly, while the “out” C-helix position is unchanged in the drug-bound structure compared to apoCdk2 (Figure 5c), the position of the chloro group on the 4-Cl-styryl in the drug would clearly clash with the “in” conformation of the C-helix in the active Cdk2-CycA dimer (Figure 5d), and the small hydrophobic pocket occupied by the 4-Cl-styryl is to large extent occluded in the heterodimer structure (Figure S4). These clashes explain the incompatibility of MC14 and CycA binding and why we observe no CycA association when Cdk2 is preincubated with drug and vice-versa.

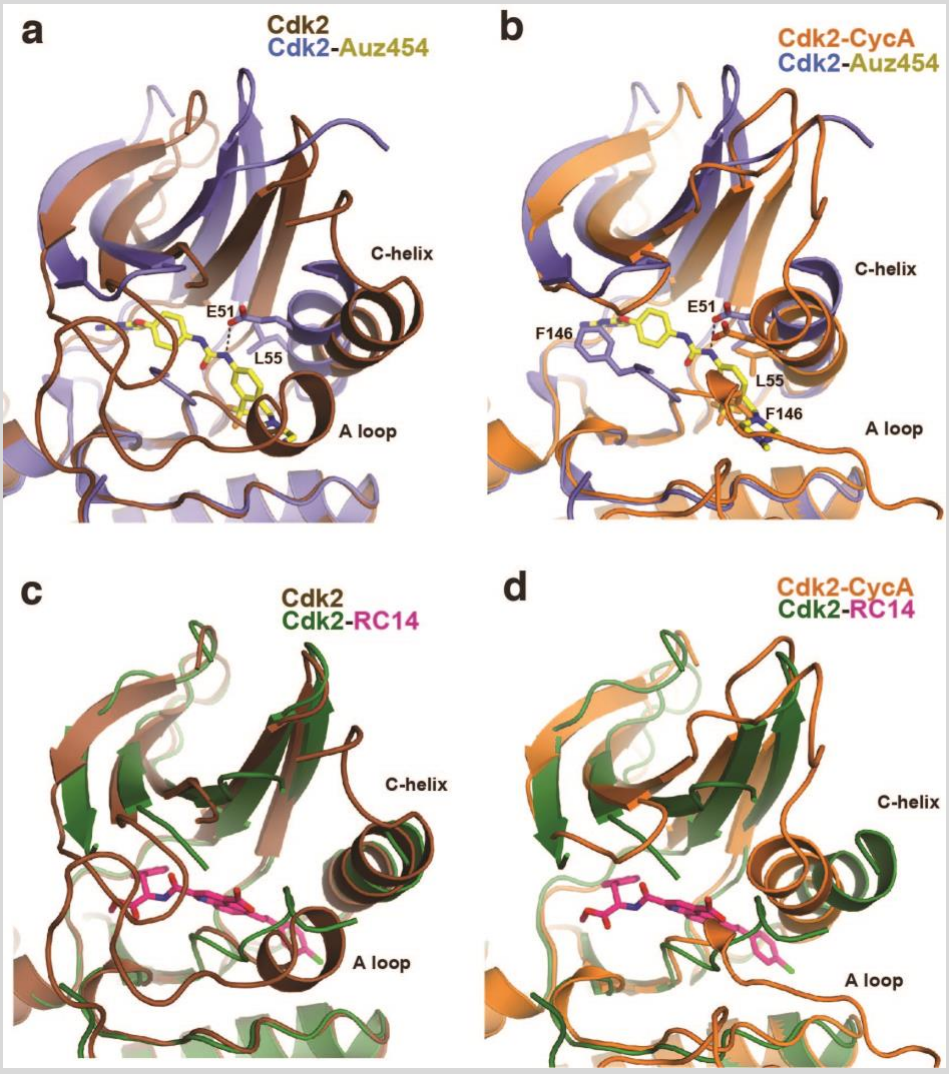

Figure 5: CCAIs impose distinct structural perturbations to influence CycA binding kinetics. Structure of Cdk2-AUZ454 (PDB: 5A14) aligned with (a) apoCdk2 (PDB: 1HCK) and (b) Cdk2-CycA (PDB: 1FIN). Structure of Cdk2-RC14 determined here bound with (c) apoCdk2 and (d) Cdk2-CycA.

2.5 Discussion

We describe here a method for direct measurement of Cdk-cyclin binding kinetics and affinity using BLI. Benefits of this approach include the high throughput, the low protein reagent requirements, and the ability to directly observe the dissociation process. Our studies

demonstrate that Cdk inhibitors can affect cyclin assembly through different mechanisms that impact both the association and dissociation rates. The Type I inhibitors tested, dinaciclib and BMS265246, increased affinity by decreasing k_d. Our observation is consistent with the previous discovery of an allosteric network that couples binding of Cdk2 ATP-site inhibitors and CycA. Interestingly, we do not observe any influence of ATP or ATP-g-S. This result suggests that other contacts made by Type I inhibitors drive the coupling to the CycA binding site. In contrast to Type I inhibitors, we found that CCAIs overall increase K_d, reducing affinity of CycA to Cdk2, but vary in their modes of how they affect the rate constants k_a and k_d. When Cdk2 is bound by the Type II inhibitor AUZ 454, we observed an increase in both k_a and k_d, while another compound MC14 inhibited CycA association when bound. These effects arise through the effect of the compounds on the conformations of the C-helix and A-loop, the two primary structural elements that couple CycA binding to increased catalytic activity.

Previous approaches have exploited a cyclin-mediated change in fluorescence of Cdk2-bound MANT(N-Methylanthraniloyl)-ATP to measure k_{obs} for the cyclin association step[20,22]. By analyzing the dependence of k_{obs} on cyclin concentration, the dissociation rate constant k_d and binding constant K_d could be indirectly determined. The affinity we measure here for CycA (K_d = 1.9 $\pm$0.8 nM) is 25-fold tighter than reported in two MANT-ATP studies (~50 nM)[14,28]. We have considered two possible reasons for this discrepancy, which relate to an advantage and disadvantage of the BLI assay respectively. First, to achieve sufficient signal, MANT-ATP measurements were necessarily made at CycA concentrations in the range of 100 nM – 1000 nM, and therefore determining k_d from the ligand concentration dependence of k_{obs} (k_{obs} = k_a[CycA] + k_d) required linear regression analysis under conditions in which k_a[CycA] is ~100-1000x greater than k_d. The direct measurement of k_d in the BLI experiment circumvents this large extrapolation to the y-intercept that is required in the MANT-ATP data analysis and is potentially error prone. On the other hand, a weakness of the BLI approach in our experiments is that the slow cyclin dissociation introduces challenges to measuring k_d. As noted, apart from

the experiments using AUZ 454, we could only reliably fit the data assuming that the response signal returns to zero; however, as seen in those AUZ 454 experiments, it is more likely that the signal returns to a non-zero baseline from an effect such as nonspecific protein aggregation on the biosensor. As a result, we believe our k_d values may be underestimated as smaller than the true values, which is consistent with us measuring a tighter K_d. It should also be noted that one MANT-ATP study showed a rapid initial increase in fluorescence, which was attributed to cyclin association with k_a 100-fold greater than our measurement[14,28]. We did not observe such an initial rapid association event using BLI.

Increasing evidence points to potential advantages of Cdk2 inhibitors that target inactive monomer Cdk2 rather than the active Cdk2-CycA dimer. First, it has been found that several ATP-site orthosteric inhibitors achieve greater selectivity for Cdk2 over Cdk1 upon binding the inactive conformation[23]. Second, if targeting the inactive Cdk2 monomer inhibits cyclin association, (i.e. how we define CCAIs), the resulting redistribution of Cdk-cyclin complexes in the cell may generate additional outputs beyond Cdk2 inhibition. For example, we and others have found that palbociclib can indirectly inhibit Cdk2 by inducing the formation of Cdk2 complexes including CIP/KIP protein inhibitors[20,25]. Our data suggest that CCAIs achieve CycA inhibition through different kinetic mechanisms. For example, the Type II inhibitor AUZ 454 increases the CycA dissociation rate, and we propose this destabilization results from the small molecule occluding the most stable conformation of the CycA-bound activation loop (Figure 5b). The fact that AUZ 454 also increases the CycA association rate suggests the compatibility of AUZ 454 and CycA in a ternary complex with Cdk2. However, this enhancement of association also results in only a maximum ~10-fold decrease in affinity under saturating conditions of drug. In contrast, MC14 completely blocks CycA association under saturating conditions and appears mutually exclusive with CycA in a complex with Cdk2 (Figures 3c and 4b). The fact that MC14 cannot bind preformed Cdk2-CycA dimers and enhance their dissociation has implications for potential effects of such a compound in the cell. For such a

molecule to be efficacious, it would have to access Cdk2 at a time in the cell division cycle, for example at the end of mitosis and early G1, when cyclin concentrations are low. We anticipate that the BLI assay described here will facilitate future inhibitor design through providing a better understanding of how Cdk inhibitors interact with and perturb Cdk-cyclin binding.

2.6 Methods

Protein expression and purification

GST-Cdk2 was expressed from a PGEX vector in BL21-DE3 *E. Coli* for 16 hrs at 20 °C using 1 mM IPTG for induction. Cells were pelleted by centrifugation and lysed using an Emulsiflex C3 cell disruptor (Avestin) in a buffer containing 25 mM Tris pH 8.0, 200 mM NaCl, 1 mM DTT, and 1 mM PMSF. The protein was then purified using Glutathione Sepharose 4B (Cytvia) affinity and anion exchange (Source Q, Cytvia) chromatography. Following elution from the anion exchange column, protein was cleaved overnight with 1% GST-TEV by mass and passed back over the glutathione sepharose column to remove free GST and GST-TEV enzyme. Cdk2 was then concentrated for final purification using a Superdex 75 (Cytvia) size-exclusion chromatography column equilibrated in 25 mM Tris pH 8.0, 200 mM NaCl and 1 mM DTT. Protein eluted as a single peak and was aliquoted and stored in 10% glycerol. GST-CycA (CycA1, residues 173-465) was purified similarly to Cdk2. To generate Cdk2 phosphorylated on its activation loop, GST-Cdk2 was co-expressed with an untagged yeast Cdk activating kinase and purified similar to as described for unphosphorylated Cdk2[3].

To generate biotinylated Cdk2, we used sortase labeling as described[40], utilizing the N-terminal glycine that is left following TEV cleavage. 500 μg of Cdk2 was reacted with 7 μg of a synthetic biotin-LPETGG peptide and a final concentration of 5 μM purified His-tagged sortase in a final reaction volume of 500 μL. The reaction was incubated for 18 hrs at 4°C. Following the reaction,

the Cdk2 was purified again by passing over a Ni^{2+}-NTA and Superdex 75 columns and stored as above.

Inhibitor compounds

AUZ 454, AZD5438, BMS265246, dinaciclib, HHT, and palbociclib were purchased from Selleckchem.com. MC14 was synthesized using methods previously described[35].

Biolayer Interferometry (BLI)

BLI experiments were performed using an eight-channel Octet-RED96e (Santorius). Experiments were performed in an assay buffer containing 25 mM Tris pH 8.0, 150 mM NaCl, 1 mM DTT, 2 mg/mL BSA, and 0.2% (v/v) Tween. Samples were formatted in a 96-well plate with each well containing 200 mL. For each experiment, we used eight streptavidin biosensor tips (Santorius) that were loaded with biotinylated Cdk2 ligand and then dipped into CycA analyte at varying CycA concentration or drug concentration. The ligand concentration at loading was 750 ng/mL for unphosphorylated Cdk2 (both GST and biotin labeled) and 1000 ng/mL for phosphorylated Cdk2. All experiments were accompanied by reference measurements using unloaded streptavidin tips dipped into the same analyte-containing wells. Experiments in which analyte concentration was varied also contained a zero-analyte reference. Data were processed and fit using Octet software, version 7 (Santorius). Before fitting, all datasets were reference-subtracted, aligned on the *y* axis through their respective baselines, aligned for interstep correction through their respective dissociation steps, and finally smoothened using Savitzy–Golay filtering. In a particular experiment, each of the sensorgrams corresponding to a different concentration of analyte or drug was fit locally using a 1:1 binding model. The first 300 seconds of association and 400 seconds of dissociation were used in the fit. In experiments in which the CycA concentration was varied, the rate and dissociation constants were averaged across the set of sensorgrams and the replicate experiment sensorgrams (14 sensorgrams in total). In the dose response experiments,

averages were takes across three replicates at each drug concentration, and the reported K_i values are averages of the K_i values determined by fitting each of three replicates. K_i was calculated using the equation $K_i = IC_{50} / (IC_{50}/[CycA] + 1)$, where IC_{50} is the fit value for the dose response curve determined using GraphPad Prism and [CycA] is the CycA concentration used in the experiment (125 nM).

Isothermal titration calorimetry (ITC)

ITC was performed with a MicroCal VP-ITC system. Purified Cdk2 was concentrated and dialyzed into a buffer containing 25 mM Tris (pH 8.0), 150 mM NaCl, and 1 mM DTT. 300 µM was titrated into HHT (30 µM) at 25 ˚C. The HHT was diluted from a 10 mM DMSO stock into the dialysis buffer and loaded into the cell. The background control experiment was performed titrating Cdk2 into buffer containing the same amount of DMSO as present in the HHT experiment. Data are presented using the MicroCal Origin software package.

X-ray crystallography

Cdk2 was crystallized following size-exclusion chromatography by the sitting drop method at 22 °C. Unliganded Cdk2 crystals were grown by mixing 1 ml of protein (10 mg/ml) with an equal volume of reservoir solution (0.2M NaCl, 100 mM MES pH 6.0, and 20% PEG 6000). Following growth, crystals were incubated overnight with 1 mM MC14 dissolved in mother liquor supplemented with 15% glycerol before flash freezing them in liquid nitrogen. Data were collected from a single crystal at the Advanced light source (ALS) Beamline 5.0.1 at 100 K. Diffraction data from the Cdk2-MC14 soaked crystals were indexed using XDS[44] and integrated and scaled using AIMLESS[45] in the CCP4 program suite[46]. The protein crystallized in $P2_12_12_1$ space group and the final structure contains one molecule of Cdk2 bound to MC14 in the asymmetric unit. Unliganded Cdk2 (PDB: 4EK3) was used as a search model in molecular replacement calculations using Phaser[47]. The Phenix suites was used for structure refinement[48]. All reflections were used for refinement except for 5% excluded for R_{free}

calculations. The structural model was revised in real space with the program COOT[49] based on sigma-A weighted 2Fo-Fc and Fo-Fc electron density maps. The final refinement statistics are given in Table S1. The structure factors and coordinates of the Cdk2-MC14 complex crystal structure were deposited in the Protein Data Bank under accession number 8CUR.

Chapter 3

Structural Characterization of a Unique Cdk4-CycD Docking Sequence in Rb that Promotes Rb Inactivation

Proper regulation of the cell cycle is highly important and is maintained through a variety of quality restriction points that evaluate the health of the cell before it enters the next phase. Coordination between phases occurs through a variety of proteins. Rb represses the transcription factor E2F by binding and preventing it from activating transcription. This repressive complex is key for halting the cell in the G1 phase. When the cell is prepared to enter S phase, cyclin-dependent kinase 4 (Cdk4) and its binding partner cyclin D (CycD) phosphorylates Rb causing inactivation and release of E2F to start transcription through downstream cell cycle genes responsible for S phase entry. Components of the Cdk4-Rb-E2F pathway are commonly deregulated in cancer; thus, the control of the G1/S phase transition is necessary for understanding cancer cell proliferation. However, it is currently unknown how this phosphorylation mechanism occurs between Rb and Cdk4-CycD. Understanding how this control is tightly regulated is essential to be able to prevent or treat when mutations lead to aberrant Cdk4 activity, especially since it can lead to lung cancer diseases.

Rb interacts with a variety of Cdk and cyclin complexes, but the initial phosphorylation necessary for its inactivation is performed by Cdk4-CycD[50]. Unlike other Cdk complexes such as Cdk2-CycA, which are thought to phosphorylate many substrates, Cdk4-CycD appears to have high specificity for Rb and its pocket protein family members, p107 and p130[51]. Residue Ser780 in Rb is phosphorylated by Cdk4-CycD and is unable to be phosphorylated by other Cdks indicating Cdk4-CycD requires specific sequence motifs for catalysis[51,52]. Cdk4-CycD is also unique in that its structure revealed that CycD binding is not sufficient to induce the active conformation of the kinase domain[53,54]. In particular, the CycD interface does not result in a

rearrangement of the activation helix (C-helix). This suggests that additional contacts may be required to push Cdk4 into the final active kinase conformation. As Rb phosphorylation catalyzes progression through the G1-S phase transition, I study Rb inactivation by Cdk4-CycD through a unique docking site on Cdk4-CycD complex will allow us to understand the mechanism of Rb inactivation. Observing this mode of regulation would explain the specificity of the enzyme and reveal a potential novel mechanism for inhibition, namely blocking Rb docking. Recent studies suggest a docking sequence in the C-terminal region of Rb, as an L901Q mutation disrupted Rb phosphorylation *in vitro* and deletion of this C-terminal region resulted in reduced Rb phosphorylation by Cdk4/6-CycD in a cell cycle Cdk-Cyc panel[55]. This site lies in the far C- terminus of RbC distal to the phosphorylation sites. Surprisingly, the sequence surrounding L901 does not contain the RxLF motif that has been well characterized as a CycA binding sequence[53]. This has alluded to the far C-terminus of Rb of about 30 amino acids long, we are calling Rbdock, interacts with Cdk4-CycD to provide an additional scaffold for the substrate and allosteric conformational change to Cdk4 that alters it into a canonical active kinase[56]. When Rb becomes phosphorylated by the Cdk4-CycD complex, a conformational change occurs that causes the release of E2F, allowing transcription and transition into the S phase[3]. Thus, it is fundamental to understand how regulation occurs in the event of losing cell cycle control[3,57].

From the prediction that Rbdock forms a helical structure, we designed mutations and in collaboration with Jan Skotheim at Stanford University and they performed kinase assays that indicate how activity of Cdk4-CycD changes upon varying constructs of Rb on subsequent substrates to determine how Rbdock association with Cdk4-CycD medites Rb phosphorylation and inactivation. Rb phosphorylation heavily decreased by Cdk4-CycD when the helix region of Rbdock (residues 890-920) is truncated, but not by other Cdk-Cyc complexes, indicating the specificity of Cdk4-CycD to Rbdock. Listed as a co-author, these data were accepted into Molecular Cell[55].

The phosphorylation mechanism of Rb by Cdk4-CycD is currently unknown and using structural and biochemical approaches to study their association and gain insight into the regulation of G1/S phase. I hypothesize that Cdk4-CycD specifically binds this region, and that this association is critical for inducing the active conformation of the kinase. Solving the Rb-Cdk4-CycD architecture in complex would reveal what guides the interaction specificity, the phosphorylation mechanism, and potential inhibitors to target this specific interface to improve on current Cdk-targeting therapeutics.

My preliminary data support the hypothesis that the sequence surrounding residue L901 has some alpha helical content and binds Cdk4-CycD. Elucidating the structure and specific binding region of Rb on the Cdk4-CycD interface would allow us to understand the mechanism of phosphorylation and how this G1-S phase transition is controlled. Moreover, demonstrating specific interactions would allow for the development of therapeutics that would allow us to control the cell cycle in the event of misregulation. I hypothesize that a conformational change induced by Rb binding properly structures the kinase active site by moving the C-helix to its proper active position. I propose to determine this novel mode of Cdk-cyclin recognition. For this reason, I propose to map the Rb-Cdk4-CycD interface and study the mechanism of Rb phosphorylation to inform the development of an inhibitor that has the specificity to target this interaction in a controlled manner[1,56].

3.1 Characterizing the interaction between Rbdock and Cdk4-CycD

I performed studies to validate the Rbdock association with Cdk4-CycD and to demonstrate the feasibility of determining an Rb-Cdk4-CycD complex structure. I began with expression and purification of several truncated Rbdock constructs that were expressed in *E. coli*. I expressed Cdk4-CycD using a baculovirus vector in *Sf9* insect cells. Recombinant proteins were purified

using affinity and ion exchange chromatography, and I assayed binding using Isothermal Titration Calorimetry (ITC) as a quantitative method and eliminated the need for tagging proteins with a fluorescent probe or other type of marker. ITC can give dissociation constants ranging from 10 nM to 100 μM. Considering that kinase docking interactions typically involve short sequences in target substrates, I expect that the sequence already tested may be sufficient. However, I expect that longer Rb constructs may have additional interactions mediated by the RxLF sequence. Preliminary data demonstrate binding of an Rbdock truncation ranging from residues 890-920 with low micromolar affinity (K_d = 13 μM) to Cdk4-CycD, that motivated future experiments to define the Rb region that forms the interface with Cdk4-CycD (Figure 6A). A previous graduate student in the lab has shown that Cdk4-CycD forms a trimer complex with p27 and is recurrent with *in vivo* experiments[58]. As a result, we tested if Rbdock can bind the Cdk4-CycD-p27 trimer by ITC (Figure 6B). The crystal structure of the p27-Cdk4-CycD1 trimer show the RxLF motif of p27 interacts with the MVRIL cleft of CycD1, suggesting that Rbdock may bind in an allosteric site outside of p27 interactions[58]. Indeed, the results indicate that Rbdock can still weakly bind the trimer giving insight that the

region of Rbdock binding in Cdk4-CycD is an area not occluded by p27, either on the kinase or the cyclin binding partner.

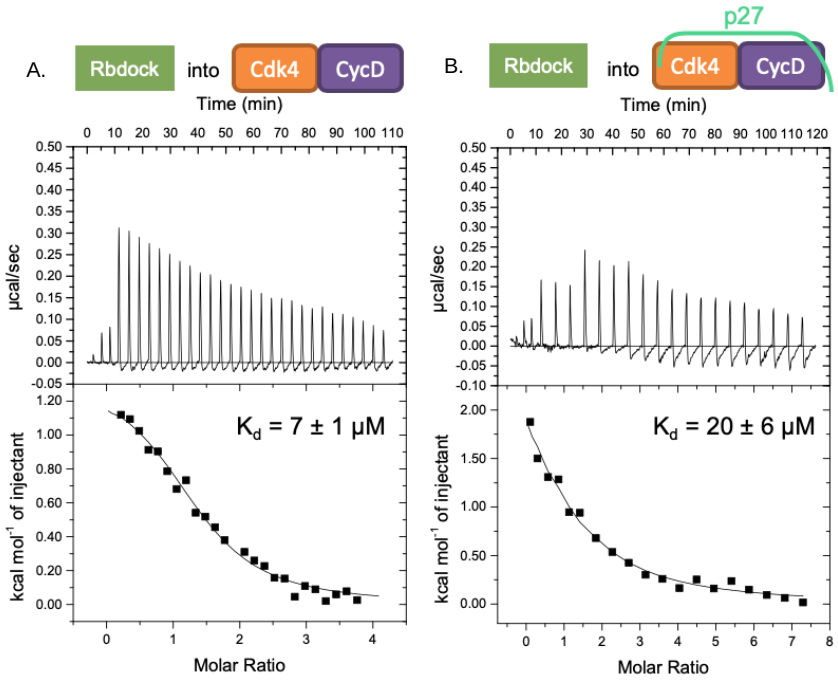

Figure 6. **Isothermal Titration Calorimetry (ITC) of Rbdock into Cdk4-CycD and p27-Cdk4-CycD** (A) Binding of Rbdock to Cdk4-CycD. (B) Rbdock weakly binds p27-Cdk4-CycD trimer complex.

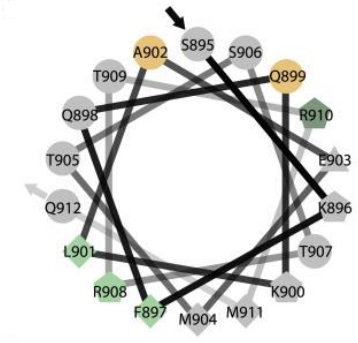

Figure 7. **Alpha helical wheel prediction for Rbdock.**

ITC Data revealed binding affinity of Rbdock to Cdk4-CycD led us to believe that these interactions take place through short motifs. It is known that upon protein-protein interactions intrinsically disordered regions of protein adopt secondary structure upon association with other proteins[59]. This led us to explore the propensity of secondary structure of the far Rb C-terminus. The use of a secondary structure prediction tool suggests the Rb docking sequence adopts an unpredicted alpha helical structure (Figure 7). I performed Circular Dichroism (CD) to test for the presence of secondary structure in the docking region of Rb (Figure 8). Intriguingly, CD data demonstrate the presence of alpha helical content in what was originally thought as a completely disordered portion of Rb. Figure 8 illustrates data from Rbdock wildtype (WT) residues 890-920 against a

fitted curve (65% disordered, 35% helix) and a disordered poly-L-lysine control. As suggested by the fit curves, these data exhibit the presence of alpha helical structure, rather than complete disordered sequence. The data are consistent with the Rb docking sequence having helical propensity in solution. The presence of a structured Rbdock supports our hypothesis of Rb docking to Cdk4-CycD through interaction of their structured domains[55].

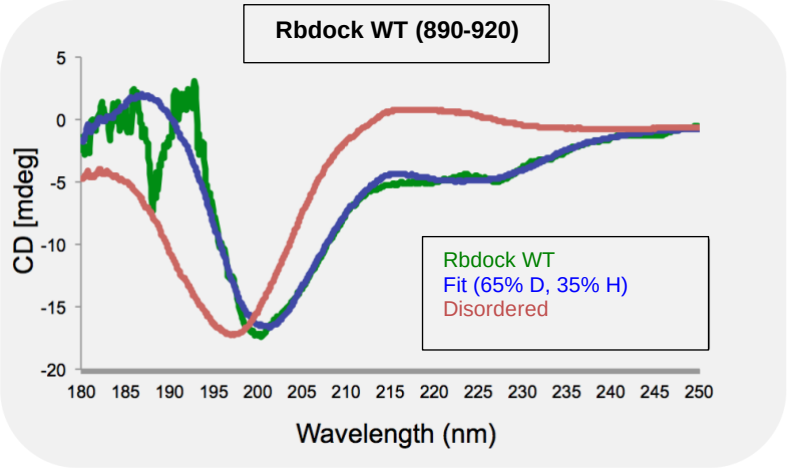

Figure 8. **Circular Dichroism (CD) of Rbdock.** Data show some structured alpha helix, in what was originally thought as a completely disordered in the far C-terminus of Rb.

An obstacle that I faced was efficiently obtaining large quantities of Cdk4-CycD from *Sf9* insect cells required for ITC, I explored other binding assays to quantify and demonstrate protein-protein interactions between Rbdock and Cdk4-CycD. I tried to obtain binding affinities through a difference technique called fluorescence polarization (FP) as the needed protein quantities are far less than that of ITC, despite the need for an additional labeling step with a fluorescent tag. For the FP assay, I fluorescently labeled Rbdock via sortase reaction with the fluorescent marker, fluorescein. The sortase reaction involves labeling a fluorophore or probe of choice onto an N-terminal glycine residue[32]. When this fluorescently labeled Rbdock is unbound in the assay, it will tumble fast, and the FP ratio will be low; when Rbdock is bound to Cdk4-CycD forming a much larger complex, it tumbles slowly and has a high FP ratio, indicative of binding.

After purification of the fluorescein labeled Rbdock, I performed FP using Rbdock (residues 890-920) and with either the kinase complexes Cdk4-CycD or Cdk2-CycA (Figure 9). We worked with Cdk2-CycA as an additional model because it is a similar kinase to Cdk4-CycD and feasible to purify large amounts from *E. coli* that also served as a negative control for Rbdock specificity to Cdk4-CycD. We thought maybe the fluorescein tag may be blocking any binding interface Rbdock may have with Cdk4-CycD leading us to use Rb129 (residues 866-928) that was slightly larger and gave a linker between the fluorophore and where the binding interface may be. The FP results of Rb129 still indicate nonspecific binding with Cdk4-CycD, as well as with Cdk2-CycA due to both kinase complexes being able to bind the negative control labeling probe lacking the Rb C-terminus (Figure 9). There is also a potential risk in that the purification process cannot separate fluorescein labeled Rb129 versus unlabeled Rb129 due to the small size of fluorescein, which may lead to the inability to reach saturation. Since FP seemed to give more issues, we utilized a new BLI technique at the time that was introduced into the MSFCF called BLI as an orthogonal method.

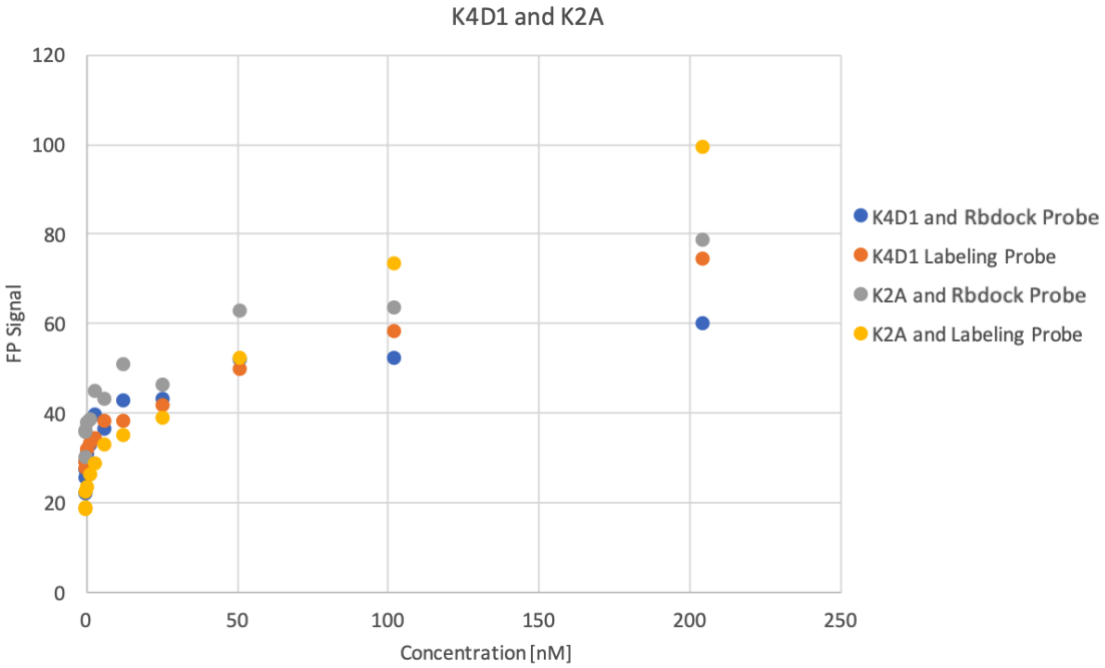

Figure 9. **Fluorescence polarization (FP) assay to test binding of Rbdock to Cdk4-CycD or Cdk2-CycA.** Cdk4-CycD1 (K4D1) and Cdk2-CycA (K2A) show binding to both Rbdock and the control labeling probes.

I used BLI to test binding between GST-tagged Rbdock and Cdk4-CycD and Cdk2-CycA using anti-GST biosensors to immobilize the GST-Rbdock onto the tip. An immobilization scouting assay was performed and found an optimal loading concentration of GST-Rbdock to be 150 ng/mL onto the sensor (not shown). During the association step with Cdk4-CycD (step 4 in Figure 10) of BLI, Rbdock binding does not reach saturation, further indicating the issue of nonspecific binding and giving an unreliable K_d (Figure 10). Similar data was seen with Cdk2-CycA. To remedy this, we did a blocking step with free-GST at 1 μM and optimized for buffer conditions to include 0.2% tween and 2 mg/mL BSA to retrieve correct K_d values (not shown). Similar to what was observed in FP, BLI also gave a large margin of nonspecific binding due to hydrophobicity and the amount of time I was spending troubleshooting FP and BLI, I decided to move forward with ITC experiments from now on.

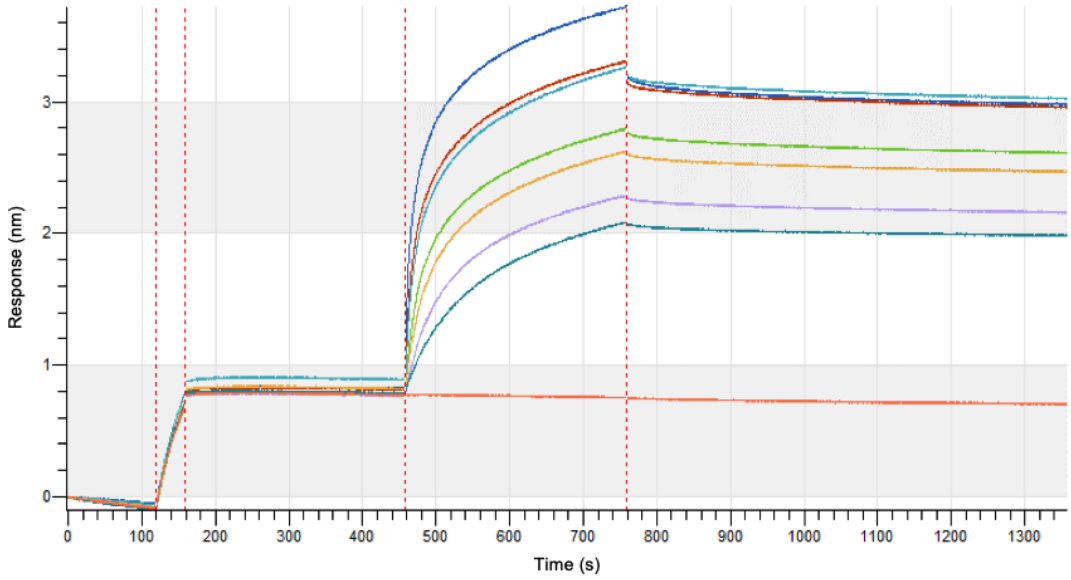

Figure 10. **A raw sensorgram of a Biolayer interferometry (BLI) assay using anti-GST biosensors.** GST-Rbdock (ligand) loaded at 150 ng/mL dipping into varying concentrations of Cdk4-CycD1 (analyte).

We have also been exploring Cdk6-CycD, a homolog of Cdk4, and like Cdk4-CycD, Cdk6-CycD can be expressed recombinantly in insect cells. Using Cdk6 gives us another opportunity to study Rbdock interaction at the G1-S phase during the phosphorylation mechanism. We

performed ITC experiments using Cdk6 to test for Rbdock binding (Figure 11). We expected to see that Rbdock binds the Cdk6-CycD-p27 trimer, indicating that with the Cdk6, Rbdock still binds where p27 is not. Figure 11A is the buffer control and Figure 11B is the experiment in which we titrated in Rbdock into Cdk6-CycD-p27 trimer. Interestingly, the buffer is giving what we initially thought of as background noise due to buffer differences. After repeating buffer conditions for both samples, both ligand and complex are in the same buffer solutions. For that reason, we believe that Rbdock does not bind Cdk6-CycD-p27 trimer as we expect. This data contradicts our initial thoughts of Rbdock binding allosterically on the cyclin and can lead us to believe that Rbdock may bind on the kinase rather. Being that the trimer complex is prevalent in cells, this gives more reason that cell-based experiments should be done with Rbdock. Although, Cdk6 is a homolog to Cdk4 there is a large discrepancy between the two kinases that may explain why no interaction was detected via ITC. Studies have shown the activation of Cdk6 by Cdk-Activating Kinase (CAK) is efficient in the absence of cyclin, whereas it is required for activation of Cdk4 by CAK (Bockstaele 2009). This may suggest that Rbdock is not essential in Cdk6 complexes as it does not require any additional contacts for proper kinase activation.

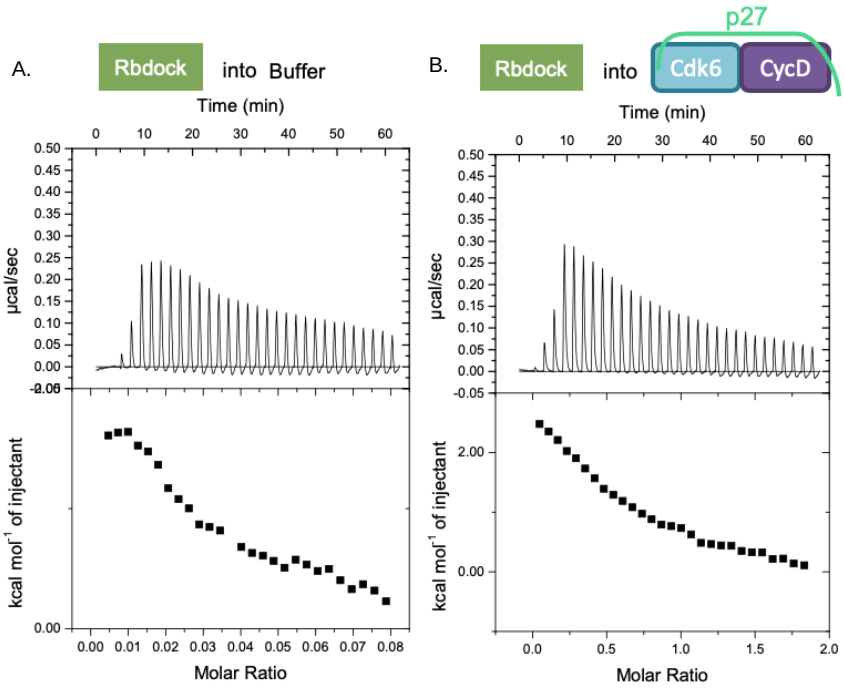

Figure 11. **ITC of Rbdock into p27-Cdk6-CycD** (A) Buffer control, Rbdock into buffer. (B)

In parallel with conducting ITC experiments, I have been setting crystal trays to determine the structure of Rb docking to Cdk4-CycD. In summary, I have set crystal trays of the following using the drop setting robot with commercial screens: Cdk4-CycD at 10 mg/mL and Rbdock (trans-), p27-Cdk4-CycD at 12 mg/mL and Rbdock (trans-), Cdk2-CycA at 15 mg/mL and Rbdock (trans-), Cdk6-CycD 10 mg/mL and Rbdock (trans-) in a variety of commercially available crystallization buffer screens with Rbdock at 5 molar excess. The crystallization buffer screens used were ProPlex, PACT *premier*, and JCSG-*plus* from Molecular Dimensions. Crystals did not grow with Rbdock-Cdk4-CycD in any of the screens. The low micromolar binding affinity that was quantified from ITC may be too weak to form a complex capable of crystal growth.

We look to Cdk2-CycA as a model for Rbdock binding because large quantities can be efficiently expressed in *E. coli* cells and crystallizes efficiently. Crystal trials that were set of Rbdock-Cdk2-CycA did grow in the ProPlex screen. Approximately, 13 of these crystals were looped and frozen in the reservoir solution with 20% glycerol. With the expertise of our crystallographer, Sarvind Tripathi, we shot our crystals remotely at the Advance Photon Source (APS) in Illinois. We collected data on two crystals that diffracted. One diffracted at 6.9Å in the buffer condition 0.1M sodium citrate pH 5, 0.1M MgCl2, and 15% PEG 4000. Another crystal diffracted at 2.8 Å in the buffer condition 0.1M sodium HEPES pH 7.5, 0.1M MgCl2, and 10% PEG 4000. In the 2.8 Å crystal structure, the unit cell only showed Cdk2-CycA alone and not in complex with Rbdock.

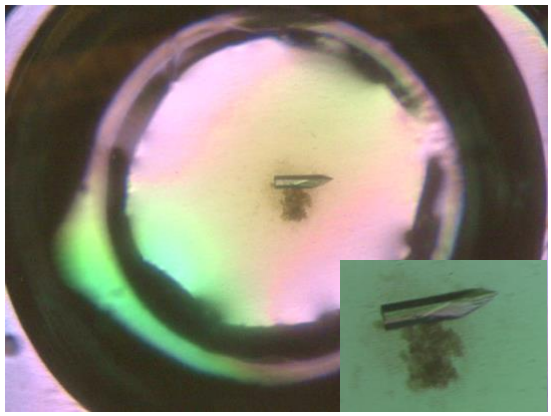

Figure 12. **Crystal of Cdk2-CycA**. Crystal diffracted at 2.8 Å that did not show Rbdock in the electron density.

Although the structure did not show RbC bound to Cdk2-CycA, it gave valuable information on crystallization conditions that can be optimized for going forward.

Rbdock variants were also explored in the attempt to promote higher binding affinity that increase crystal formation. The most exciting was obtaining an Rbdock stapled helix construct from collaborators. The stapled helix of Rbdock was ordered to contain a "staple," a bridge that keeps the Rbdock in an alpha helical secondary structure. We expect this stapled Rbdock helix to help with crystallization. I was able to set crystal trays of the stapled helix with Cdk4-CycD; unfortunately, it did not generate any observable crystal growth.

Research aims have shifted slightly to overcome the inability to grow protein crystals for x-ray crystallography, but this shift in perspective still contributes to the continued effort in developing of more targeted Cdk inhibitors.

3.2 Methods

Protein expression and purification

Recombinant Cdk4-CycD was expressed from a pFastBac dual vector from *Sf9* cells through the generation of bacmid and viruses using the Bac-to-Bac™ baculovirus expression system. Cdk4 was expressed as a GST-fusion protein while CycD was co-expressed with no tag. Expression took place at 27°C shaking for 3 days following viral infection and cells were pelleted by centrifugation at 4°C and from this point forward all reagents were kept cold either at 4°C or on ice. Lysate was sonicated in a buffer containing 25 mM Tris pH 8.0, 150 mM NaCl, 1 mM DTT, and 1 mM protease inhibitor (PI) cocktail (Sigma), and centrifugated at 19,000 RPM for 45 minutes to pellet insoluble fraction from the soluble fraction. Target proteins were in the soluble fraction and was purified using Glutathione Sepharose 4B (Cytvia) affinity in batch

method and anion exchange (Source Q, Cytvia) chromatography. Following elution from the anion exchange column, protein was cleaved overnight with 1% GST-TEV by mass and passed back over the glutathione sepharose column to remove free GST and GST-TEV enzyme. Cdk2 was then concentrated for final purification using a Superdex 75 (Cytvia) size-exclusion chromatography column equilibrated in 25 mM Tris pH 8.0, 150 mM NaCl and 1 mM DTT. Protein eluted as a single peak and was aliquoted and stored in 10% glycerol. The trimer complex p27-Cdk4-CycD was reconstituted by adding recombinantly expressed p27 from *E. coli* to purified Cdk4-CycD and further purified using Superdex 75. Homolog Cdk6-CycD and p27-Cdk6-CycD was purified as described above. Rbdock and Cdk2-CycA were expressed as a GST-fusion protein in *E. coli* and purified similarly.

To generate fluorescein labeled Cdk4 and Cdk2 for FP, we used sortase labeling as described[40], utilizing the N-terminal glycine that is left following TEV cleavage. 500 μg of kinase was reacted with 7 μg of a synthetic biotin-LPETGG peptide and a final concentration of 5 μM purified His-tagged sortase in a final reaction volume of 500 μL. The reaction was incubated for 18 hrs at 4°C. Following the reaction, the labelled protein was purified again by passing over a Ni^{2+}-NTA and Superdex 75 columns and stored as above.

Isothermal Titration Calorimetry (ITC)

Dissociation constants were obtained using a Micro Cal VP-ITC at 15°C. For Rbdock binding experiments, Cdk4-CycD and p27-Cdk4/6-CycD, were dialyzed overnight in a buffer containing 25 mM Tris pH 8.0, 150 mM NaCl, and 1 mM BME. Kinase complexes were titrated with xx mM Rbdock dissolved in the same dialysis buffer.

Circular Dichroism (CD)

CD spectra were recorded using a Jasco J-1500 CD spectrometer. Samples contained 30 mM recombinant Rb 890-920 in a buffer containing 25 mM sodium phosphate and 100 mM NaCl (pH 6.1). The data were fit by calculating a weighted average of reference spectra measured for poly-L-lysine, which adopts known different secondary structures depending on pH and temperature[60].

Fluorescence polarization (FP)

Labeling probes were synthesized and ordered by Genscript. Fluorescein labeled Cdk4 and Cdk2 were labeled as mentioned above. 20 nM peptide was mixed with varying concentrations of either Cdk4-CycD or Cdk2-CycA kinase complex in a buffer containing 40 mM Tris pH 8, 150 mM NaCl, 1 mM DTT, and 0.05% (v/v) Tween-20. Twenty microliters of the reaction were used for the measurement in a 384-well plate using a Perkin-Elmer EnVision plate reader. Data collected were done in triplicate.

Biolayer interferometry (BLI)

BLI experiments were performed using an eight-channel Octet-RED96e (Santorius). Experiments were performed in an assay buffer containing 25 mM Tris pH 8.0, 150 mM NaCl, 1 mM DTT, 2 mg/mL BSA, and 0.2% (v/v) Tween. Samples were formatted in a 96-well plate with each well containing 200 mL. For each experiment, we used eight anti-GST biosensor tips (Santorius) that were loaded with GST-Rbdock ligand and then dipped into Cdk4-CycD analyte at varying analyte concentrations. Since Rbdock was immobilized onto the anti-GST biosensor using the affinity tag, Rbdock was not cleaved and purified as described above. The ligand concentration at loading was 150 ng/mL for GST-Rbdock and varying concentration for phosphorylated Cdk2. All experiments were accompanied by reference measurements using unloaded anti-GST tips dipped into the same analyte-containing wells. Experiments in which analyte concentration was varied also contained a zero-analyte reference. Data were

processed and fit using Octet software, version 7 (Santorius). Before fitting, all datasets were reference-subtracted, aligned on the *y* axis through their respective baselines, aligned for interstep correction through their respective dissociation steps, and finally smoothened using Savitzy–Golay filtering. In a particular experiment, each of the sensorgrams corresponding to a different concentration of analyte or drug was fit locally using a 1:1 binding model.

Crystallization trials

Crystal trays were set of either kinase complex Cdk4-CycD at 10 mg/mL or Cdk2-CycA at 15 mg/mL with Rbdock at 5 molar excess using the Art Robbins Instrument (ARI) Gryphon of varying ratios of screening buffer to protein at 3:1, 1:1, and 1:3, respectively. The crystallization buffer screens used were ProPlex, PACT *premier*, and JCSG-*plus* from Molecular Dimensions. After several days and weeks at 22°C crystal growth was not observed for Cdk4-CycD under screening crystallization conditions. The crystal tray with Cdk2-CycA and Rbdock did grow in the ProPlex crystallization screen in the condition 0.1M sodium citrate pH 5, 0.1M MgCl2, and 15% PEG 4000. Crystals were looped in their mother liquor with 15% glycerol before flash freezing them in liquid nitrogen. Data were collected from a single crystal at the Advanced light source (ALS) Beamline 5.0.1 at 100 K.

Bibliography

1. Cancer Genome Atlas Research, N., *Comprehensive molecular profiling of lung adenocarcinoma.* Nature, 2014. **511**(7511): p. 543-50.
2. Burkhart, D.L. & Sage, J. Cellular mechanisms of tumour suppression by the retinoblastoma gene. *Nat Rev Cancer* **8**, 671-82 (2008).
3. Dick, F.A. & Rubin, S.M. Molecular mechanisms underlying RB protein function. *Nat Rev Mol Cell Biol* **14**, 297-306 (2013).
4. Morgan, D. O., Cyclin-dependent kinases: engines, clocks, and microprocessors. *Annu Rev Cell Dev Biol* **1997,** *13*, 261-91.
5. Wood, D. J.; Endicott, J. A., Structural insights into the functional diversity of the CDK-cyclin family. *Open Biol* **2018,** *8* (9).
6. Hanahan, Douglas, and Robert A. Weinberg. “Hallmarks of Cancer: The next Generation.” *Cell*, vol. 144, no. 5, 2011, pp. 646–674.
7. Malumbres, M., Cyclin-dependent kinases. *Genome Biol* **2014,** *15* (6), 122. Morgan, D. O., Cyclin-dependent kinases: engines, clocks, and microprocessors. *Annu Rev Cell Dev Biol* **1997,** *13*, 261-91.
8. Jeffrey, P. D.; Russo, A. A.; Polyak, K.; Gibbs, E.; Hurwitz, J.; Massague, J.; Pavletich, N. P., Mechanism of CDK activation revealed by the structure of a cyclinA-CDK2 complex. *Nature* **1995,** *376* (6538), 313-20.
9. Russo, A. A.; Jeffrey, P. D.; Pavletich, N. P., Structural basis of cyclin-dependent kinase activation by phosphorylation. *Nat Struct Biol* **1996,** *3* (8), 696-700.
10. Rubin, S. M.; Sage, J.; Skotheim, J. M., Integrating Old and New Paradigms of G1/S Control. *Mol Cell* **2020,** *80* (2), 183-192.
11. Malumbres, Marcos, and Mariano Barbacid. “Cell Cycle, Cdks and Cancer: A Changing Paradigm.” *Nature Reviews Cancer*, vol. 9, no. 3, 2009, pp. 153–166.

12. Otto, T.; Sicinski, P., Cell cycle proteins as promising targets in cancer therapy. *Nat Rev Cancer* **2017,** *17* (2), 93-115.
13. Sherr, C. J.; Beach, D.; Shapiro, G. I., Targeting CDK4 and CDK6: From Discovery to Therapy. *Cancer Discov* **2016,** *6* (4), 353-67.
14. Brown, N. R.; Noble, M. E.; Lawrie, A. M.; Morris, M. C.; Tunnah, P.; Divita, G.; Johnson, L. N.; Endicott, J. A., Effects of phosphorylation of threonine 160 on cyclin-dependent kinase 2 structure and activity. *J Biol Chem* **1999,** *274* (13), 8746-56.
15. Echalier, Aude, et al. "An Inhibitor's-Eye View of the ATP-Binding Site of Cdks in Different Regulatory States." *ACS Chemical Biology*, vol. 9, no. 6, 2014, pp. 1251–1256.
16. Sánchez-Martínez, Concepción, et al. "Cyclin Dependent Kinase (CDK) Inhibitors as Anticancer Drugs: Recent Advances (2015–2019)." *Bioorganic & Medicinal Chemistry Letters*, vol. 29, no. 20, 2019, p. 126637.
17. Toogood, P. L.; Harvey, P. J.; Repine, J. T.; Sheehan, D. J.; VanderWel, S. N.; Zhou, H.; Keller, P. R.; McNamara, D. J.; Sherry, D.; Zhu, T.; Brodfuehrer, J.; Choi, C.; Barvian, M. R.; Fry, D. W., Discovery of a potent and selective inhibitor of cyclin-dependent kinase 4/6. *J Med Chem* **2005,** *48* (7), 2388-406.
18. Finn, R. S.; Martin, M.; Rugo, H. S.; Jones, S.; Im, S. A.; Gelmon, K.; Harbeck, N.; Lipatov, O. N.; Walshe, J. M.; Moulder, S.; Gauthier, E.; Lu, D. R.; Randolph, S.; Dieras, V.; Slamon, D. J., Palbociclib and Letrozole in Advanced Breast Cancer. *N Engl J Med* **2016,** *375* (20), 1925-1936.
19. Chaikovsky, A. C.; Li, C.; Jeng, E. E.; Loebell, S.; Lee, M. C.; Murray, C. W.; Cheng, R.; Demeter, J.; Swaney, D. L.; Chen, S. H.; Newton, B. W.; Johnson, J. R.; Drainas, A. P.; Shue, Y. T.; Seoane, J. A.; Srinivasan, P.; He, A.; Yoshida, A.; Hipkins, S. Q.; McCrea, E.; Poltorack, C. D.; Krogan, N. J.; Diehl, J. A.; Kong, C.; Jackson, P. K.; Curtis, C.; Petrov, D. A.; Bassik, M. C.; Winslow, M. M.; Sage, J., The AMBRA1 E3 ligase adaptor regulates the stability of cyclin D. *Nature* **2021,** *592* (7856), 794-798.

20. Guiley, K. Z.; Stevenson, J. W.; Lou, K.; Barkovich, K. J.; Kumarasamy, V.; Wijeratne, T. U.; Bunch, K. L.; Tripathi, S.; Knudsen, E. S.; Witkiewicz, A. K.; Shokat, K. M.; Rubin, S. M., p27 allosterically activates cyclin-dependent kinase 4 and antagonizes palbociclib inhibition. *Science* **2019,** *366* (6471).
21. Herrera-Abreu, M. T.; Palafox, M.; Asghar, U.; Rivas, M. A.; Cutts, R. J.; Garcia-Murillas, I.; Pearson, A.; Guzman, M.; Rodriguez, O.; Grueso, J.; Bellet, M.; Cortes, J.; Elliott, R.; Pancholi, S.; Baselga, J.; Dowsett, M.; Martin, L. A.; Turner, N. C.; Serra, V., Early Adaptation and Acquired Resistance to CDK4/6 Inhibition in Estrogen Receptor-Positive Breast Cancer. *Cancer Res* **2016,** *76* (8), 2301-13.
22. Aleem, E.; Kiyokawa, H.; Kaldis, P., Cdc2-cyclin E complexes regulate the G1/S phase transition. *Nat Cell Biol* **2005,** *7* (8), 831-6.
23. Wood, D. J.; Korolchuk, S.; Tatum, N. J.; Wang, L. Z.; Endicott, J. A.; Noble, M. E. M.; Martin, M. P., Differences in the Conformational Energy Landscape of CDK1 and CDK2 Suggest a Mechanism for Achieving Selective CDK Inhibition. *Cell Chem Biol* **2019,** *26* (1), 121-130 e5.
24. Li, Q.; Jiang, B.; Guo, J.; Shao, H.; Del Priore, I. S.; Chang, Q.; Kudo, R.; Li, Z.; Razavi, P.; Liu, B.; Boghossian, A. S.; Rees, M. G.; Ronan, M. M.; Roth, J. A.; Donovan, K. A.; Palafox, M.; Reis-Filho, J. S.; de Stanchina, E.; Fischer, E. S.; Rosen, N.; Serra, V.; Koff, A.; Chodera, J. D.; Gray, N. S.; Chandarlapaty, S., INK4 tumor suppressor proteins mediate resistance to CDK4/6 kinase inhibitors. *Cancer Discov* **2021**.
25. Pack, L. R.; Daigh, L. H.; Chung, M.; Meyer, T., Clinical CDK4/6 inhibitors induce selective and immediate dissociation of p21 from cyclin D-CDK4 to inhibit CDK2. *Nat Commun* **2021,** *12* (1), 3356.
26. Bloom, J.; Cross, F. R., Multiple levels of cyclin specificity in cell-cycle control. *Nat Rev Mol Cell Biol* **2007,** *8* (2), 149-60.

27. Heitz, F.; Morris, M. C.; Fesquet, D.; Cavadore, J. C.; Doree, M.; Divita, G., Interactions of cyclins with cyclin-dependent kinases: a common interactive mechanism. *Biochemistry* **1997,** *36* (16), 4995-5003.
28. Morris, M. C.; Gondeau, C.; Tainer, J. A.; Divita, G., Kinetic mechanism of activation of the Cdk2/cyclin A complex. Key role of the C-lobe of the Cdk. *J Biol Chem* **2002,** *277* (26), 23847-53.
29. Alvarez-Fernandez, M.; Malumbres, M., Mechanisms of Sensitivity and Resistance to CDK4/6 Inhibition. *Cancer Cell* **2020,** *37* (4), 514-529.
30. Brown, N. R.; Korolchuk, S.; Martin, M. P.; Stanley, W. A.; Moukhametzianov, R.; Noble, M. E. M.; Endicott, J. A., CDK1 structures reveal conserved and unique features of the essential cell cycle CDK. *Nat Commun* **2015,** *6*, 6769.
31. Diril, M. K.; Ratnacaram, C. K.; Padmakumar, V. C.; Du, T.; Wasser, M.; Coppola, V.; Tessarollo, L.; Kaldis, P., Cyclin-dependent kinase 1 (Cdk1) is essential for cell division and suppression of DNA re-replication but not for liver regeneration. *Proc Natl Acad Sci U S A* **2012,** *109* (10), 3826-31.
32. Santamaria, D.; Barriere, C.; Cerqueira, A.; Hunt, S.; Tardy, C.; Newton, K.; Caceres, J. F.; Dubus, P.; Malumbres, M.; Barbacid, M., Cdk1 is sufficient to drive the mammalian cell cycle. *Nature* **2007,** *448* (7155), 811-5.
33. Alexander, L. T.; Mobitz, H.; Drueckes, P.; Savitsky, P.; Fedorov, O.; Elkins, J. M.; Deane, C. M.; Cowan-Jacob, S. W.; Knapp, S., Type II Inhibitors Targeting CDK2. *ACS Chem Biol* **2015,** *10* (9), 2116-25.
34. Alexander, L. T.; Mobitz, H.; Drueckes, P.; Savitsky, P.; Fedorov, O.; Elkins, J. M.; Deane, C. M.; Cowan-Jacob, S. W.; Knapp, S., Type II Inhibitors Targeting CDK2. *ACS Chem Biol* **2015,** *10* (9), 2116-25.
35. Deng, Y.; Shipps, G. W., Jr.; Zhao, L.; Siddiqui, M. A.; Popovici-Muller, J.; Curran, P. J.; Duca, J. S.; Hruza, A. W.; Fischmann, T. O.; Madison, V. S.; Zhang, R.; McNemar, C. W.; Mayhood, T. W.; Syto, R.; Annis, A.; Kirschmeier, P.; Lees, E. M.; Parry, D. A.;

Windsor, W. T., Modulating the interaction between CDK2 and cyclin A with a quinoline-based inhibitor. *Bioorg Med Chem Lett* **2014,** *24* (1), 199-203.

36. Zhang, J.; Gan, Y.; Li, H.; Yin, J.; He, X.; Lin, L.; Xu, S.; Fang, Z.; Kim, B. W.; Gao, L.; Ding, L.; Zhang, E.; Ma, X.; Li, J.; Li, L.; Xu, Y.; Horne, D.; Xu, R.; Yu, H.; Gu, Y.; Huang, W., Inhibition of the CDK2 and Cyclin A complex leads to autophagic degradation of CDK2 in cancer cells. *Nat Commun* **2022,** *13* (1), 2835.
37. Majumdar, A.; Burban, D. J.; Muretta, J. M.; Thompson, A. R.; Engel, T. A.; Rasmussen, D. M.; Subrahmanian, M. V.; Veglia, G.; Thomas, D. D.; Levinson, N. M., Allostery governs Cdk2 activation and differential recognition of CDK inhibitors. *Nat Chem Biol* **2021,** *17* (4), 456-464.
38. Abdiche, Y.; Malashock, D.; Pinkerton, A.; Pons, J., Determining kinetics and affinities of protein interactions using a parallel real-time label-free biosensor, the Octet. *Anal Biochem* **2008,** *377* (2), 209-17.
39. Wilson, J. L.; Scott, I. M.; McMurry, J. L., Optical biosensing: Kinetics of protein A-IGG binding using biolayer interferometry. *Biochem Mol Biol Educ* **2010,** *38* (6), 400-7.
40. Theile, C. S.; Witte, M. D.; Blom, A. E.; Kundrat, L.; Ploegh, H. L.; Guimaraes, C. P., Site-specific N-terminal labeling of proteins using sortase-mediated reactions. *Nat Protoc* **2013,** *8* (9), 1800-7.
41. Parry, D.; Guzi, T.; Shanahan, F.; Davis, N.; Prabhavalkar, D.; Wiswell, D.; Seghezzi, W.; Paruch, K.; Dwyer, M. P.; Doll, R.; Nomeir, A.; Windsor, W.; Fischmann, T.; Wang, Y.; Oft, M.; Chen, T.; Kirschmeier, P.; Lees, E. M., Dinaciclib (SCH 727965), a novel and potent cyclin-dependent kinase inhibitor. *Mol Cancer Ther* **2010,** *9* (8), 2344-53.
42. Misra, R. N.; Xiao, H.; Rawlins, D. B.; Shan, W.; Kellar, K. A.; Mulheron, J. G.; Sack, J. S.; Tokarski, J. S.; Kimball, S. D.; Webster, K. R., 1H-Pyrazolo[3,4-b]pyridine inhibitors of cyclin-dependent kinases: highly potent 2,6-Difluorophenacyl analogues. *Bioorg Med Chem Lett* **2003,** *13* (14), 2405-8.

43. Schulze-Gahmen, U.; De Bondt, H. L.; Kim, S. H., High-resolution crystal structures of human cyclin-dependent kinase 2 with and without ATP: bound waters and natural ligand as guides for inhibitor design. *J Med Chem* **1996,** *39* (23), 4540-6.
44. Kabsch, W., Integration, scaling, space-group assignment and post-refinement. *Acta Crystallogr D Biol Crystallogr* **2010,** *66* (Pt 2), 133-44.
45. Evans, P., Scaling and assessment of data quality. *Acta Crystallogr D Biol Crystallogr* **2006,** *62* (Pt 1), 72-82.
46. Winn, M. D.; Ballard, C. C.; Cowtan, K. D.; Dodson, E. J.; Emsley, P.; Evans, P. R.; Keegan, R. M.; Krissinel, E. B.; Leslie, A. G.; McCoy, A.; McNicholas, S. J.; Murshudov, G. N.; Pannu, N. S.; Potterton, E. A.; Powell, H. R.; Read, R. J.; Vagin, A.; Wilson, K. S., Overview of the CCP4 suite and current developments. *Acta Crystallogr D Biol Crystallogr* **2011,** *67* (Pt 4), 235-42.
47. McCoy, A. J.; Grosse-Kunstleve, R. W.; Adams, P. D.; Winn, M. D.; Storoni, L. C.; Read, R. J., Phaser crystallographic software. *J Appl Crystallogr* **2007,** *40* (Pt 4), 658-674.
48. Adams, P. D.; Afonine, P. V.; Bunkoczi, G.; Chen, V. B.; Davis, I. W.; Echols, N.; Headd, J. J.; Hung, L. W.; Kapral, G. J.; Grosse-Kunstleve, R. W.; McCoy, A. J.; Moriarty, N. W.; Oeffner, R.; Read, R. J.; Richardson, D. C.; Richardson, J. S.; Terwilliger, T. C.; Zwart, P. H., PHENIX: a comprehensive Python-based system for macromolecular structure solution. *Acta Crystallogr D Biol Crystallogr* **2010,** *66* (Pt 2), 213-21.
49. Emsley, P.; Cowtan, K., Coot: model-building tools for molecular graphics. *Acta Crystallogr D Biol Crystallogr* **2004,** *60* (Pt 12 Pt 1), 2126-32.
50. Day, P.J., et al., *Crystal structure of human CDK4 in complex with a D-type cyclin.* Proc Natl Acad Sci U S A, 2009. **106**(11): p. 4166-70.
51. Kitagawa, M., et al. “The Consensus Motif for Phosphorylation by Cyclin D1-cdk4 Is Different from That for Phosphorylation by Cyclin A/E-cdk2.” *The EMBO Journal*, vol. 15, no. 24, 1996, pp. 7060–7069.

52. Zarkowska, Tamara, and Sibylle Mittnacht. “Differential Phosphorylation of the Retinoblastoma Protein by G1/S Cyclin-Dependent Kinases.” *Journal of Biological Chemistry*, vol. 272, no. 19, 1997, pp. 12738–12746.
53. Rubin, S.M. & Sage, J. Defining a new vision for the retinoblastoma gene: report from the 3rd International Rb Meeting. *Cell Div* **8**, 13 (2013).
54. O'Leary, B., R.S. Finn, and N.C. Turner, *Treating cancer with selective CDK4/6 inhibitors.* Nat Rev Clin Oncol, 2016. **13**(7): p. 417-30.
55. Topacio, Benjamin R., et al. “Cyclin D-CDK4,6 Drives Cell-Cycle Progression via the Retinoblastoma Protein’s C-Terminal Helix.” *Molecular Cell*, vol. 74, no. 4, 2019.
56. Pan, W., et al., *A cyclin D1/cyclin-dependent kinase 4 binding site within the C domain of the retinoblastoma protein.* Cancer Res, 2001. **61**(7): p. 2885-91.
57. Polk, A., et al., *Specific CDK4/6 inhibition in breast cancer: a systematic review of current clinical evidence.* ESMO Open, 2016. **1**(6): p. e000093.
58. Burke, J.R., Hura, G.L. & Rubin, S.M. Structures of inactive retinoblastoma protein reveal multiple mechanisms for cell cycle control. *Genes Dev* **26**, 1156-66 (2012).
59. Rubin, Seth M., et al. “Structure of the RB C-Terminal Domain Bound to E2F1-DP1: A Mechanism for Phosphorylation-Induced E2F Release.” *Cell*, vol. 123, no. 6, 2005, pp. 1093–1106.
60. Greenfield, Norma J., and Gerald D. Fasman. “Computed Circular Dichroism Spectra for the Evaluation of Protein Conformation.” *Biochemistry*, vol. 8, no. 10, 1969, pp. 4108–4116.